SUCCESSFUL SCIENTISTS ARE NOT JUST SMART.
THEY WORK SMART.
STEMCELL TECHNOLOGIES
FIND OUT HOW

The Journal of Immunology

Genome-Wide Posttranscriptional Dysregulation by MicroRNAs in Human Asthma as Revealed by Frac-seq

This information is current as of May 24, 2018.

Rocio T. Martinez-Nunez, Hitasha Rupani, Manuela Platé, Mahesan Niranjan, Rachel C. Chambers, Peter H. Howarth and Tilman Sanchez-Elsner

J Immunol published online 16 May 2018
http://www.jimmunol.org/content/early/2018/05/15/jimmunol.1701798

Supplementary Material http://www.jimmunol.org/content/suppl/2018/05/16/jimmunol.1701798.DCSupplemental

Why *The JI*? Submit online.

- **Rapid Reviews! 30 days*** from submission to initial decision
- **No Triage!** Every submission reviewed by practicing scientists
- **Fast Publication!** 4 weeks from acceptance to publication

**average*

Subscription Information about subscribing to *The Journal of Immunology* is online at: http://jimmunol.org/subscription

Permissions Submit copyright permission requests at: http://www.aai.org/About/Publications/JI/copyright.html

Email Alerts Receive free email-alerts when new articles cite this article. Sign up at: http://jimmunol.org/alerts

The Journal of Immunology is published twice each month by
The American Association of Immunologists, Inc.,
1451 Rockville Pike, Suite 650, Rockville, MD 20852
Copyright © 2018 by The American Association of Immunologists, Inc. All rights reserved.
Print ISSN: 0022-1767 Online ISSN: 1550-6606.

Downloaded from http://www.jimmunol.org/ by guest on May 24, 2018

Published May 16, 2018, doi:10.4049/jimmunol.1701798

Genome-Wide Posttranscriptional Dysregulation by MicroRNAs in Human Asthma as Revealed by Frac-seq

Rocio T. Martinez-Nunez,*,† Hitasha Rupani,†,‡ Manuela Platé,§ Mahesan Niranjan,¶ Rachel C. Chambers,§ Peter H. Howarth,†,‡,1 and Tilman Sanchez-Elsner†,1

MicroRNAs are small noncoding RNAs that inhibit gene expression posttranscriptionally, implicated in virtually all biological processes. Although the effect of individual microRNAs is generally studied, the genome-wide role of multiple microRNAs is less investigated. We assessed paired genome-wide expression of microRNAs with total (cytoplasmic) and translational (polyribosome-bound) mRNA levels employing subcellular fractionation and RNA sequencing (Frac-seq) in human primary bronchoepithelium from healthy controls and severe asthmatics. Severe asthma is a chronic inflammatory disease of the airways characterized by poor response to therapy. We found genes (i.e., isoforms of a gene) and mRNA isoforms differentially expressed in asthma, with novel inflammatory and structural pathophysiological mechanisms related to bronchoepithelium disclosed solely by polyribosome-bound mRNAs (e.g., *IL1A* and *LTB* genes or *ITGA6* and *ITGA2* alternatively spliced isoforms). Gene expression (i.e., isoforms of a gene) and mRNA expression analysis revealed different molecular candidates and biological pathways, with differentially expressed polyribosome-bound and total mRNAs also showing little overlap. We reveal a hub of six dysregulated microRNAs accounting for ∼90% of all microRNA targeting, displaying preference for polyribosome-bound mRNAs. Transfection of this hub in bronchial epithelial cells from healthy donors mimicked asthma characteristics. Our work demonstrates extensive posttranscriptional gene dysregulation in human asthma, in which microRNAs play a central role, illustrating the feasibility and importance of assessing posttranscriptional gene expression when investigating human disease. ***The Journal of Immunology*****, 2018, 201: 000–000.**

MicroRNAs are small regulatory molecules (∼22 nucleotides long) that inhibit gene expression by pairing mainly to the 3′ untranslated regions (UTRs) of their target mRNAs (1). MicroRNA effects include mRNA destabilization and inhibition of translation, with a body of literature supporting both as main effector mechanisms (2–5). The biological relevance of microRNAs expands to most cellular processes, as thousands of mRNAs contain microRNA responsive elements (MREs). Consequently, microRNA dysregulation has been demonstrated to underlie disease pathophysiological mechanisms, making microRNAs novel therapeutic targets (6).

Although the effects of individual microRNAs in disease have been explored extensively, there are fewer reports on the role of microRNAs acting as networks in this setting. We have previously shown that microRNAs dysregulated in bronchial epithelial cells (BECs) from asthmatic patients may have different effects, even opposite effects, when modulating their levels individually versus simultaneously (7). Our work and others (8) highlight the need for integrative genome-wide approaches to understand the role and importance of microRNAs in cellular and pathological processes.

Asthma is a common chronic inflammatory disease of the airways affecting ∼350 million people worldwide and with a spectrum of severity. Severe asthma (SA) is characterized by the need for or the failure to respond to high-dose glucocorticoids in conjunction with other additional controller therapies (9). The underlying mechanisms of SA remain incompletely understood, and it therefore represents a major unmet clinical need, accounting for the majority of the healthcare budget dedicated to asthma. Current therapy for asthma targets the inflammatory and smooth muscle constrictor components of the disease. Because SA patients remain uncontrolled, it is

*School of Immunology and Microbial Sciences, Medical Research Council and Asthma UK Centre in Allergic Mechanisms of Asthma, King's College London, London SE19RT, United Kingdom; †Clinical and Experimental Sciences, Faculty of Medicine, University of Southampton, Southampton SO16 6YD, United Kingdom; ‡Southampton National Institute for Health Research Respiratory Biomedical Research Unit, Southampton Centre for Biomedical Research, University Hospital Southampton National Health Service Foundation Trust, Southampton SO16 6YD, United Kingdom; §Centre for Inflammation and Tissue Repair, Department of Respiratory Medicine, Rayne Institute, University College London, London WC1E 6JF, United Kingdom; and ¶School of Electronics and Computer Science, University of Southampton, Southampton SO17 1BJ, United Kingdom

[1]P.H.H. and T.S.-E. share joint senior authorship.

ORCIDs: 0000-0003-2507-4738 (R.T.M.-N.); 0000-0002-9957-0681 (M.P.); 0000-0001-7021-140X (M.N.); 0000-0003-1370-9417 (R.C.C.); 0000-0003-1915-2410 (T.S.-E.).

Received for publication December 29, 2017. Accepted for publication April 17, 2018.

This work was supported by Medical Research Council United Kingdom Grants G0800649 (Wessex Severe Asthma Cohort), MR/K001035/1, and G0900453. Equipment (to P.H.H. and T.S.-E.) and reagent (to R.T.M.-N.) grants were from the Southampton Asthma, Allergy, and Inflammation Research Charity. R.T.M.-N. was in receipt of the Postdoctoral Career Track award from the Faculty of Medicine, University of Southampton.

The sequencing data presented in this article have been submitted to the National Center for Biotechnology Information Gene Expression Omnibus (http://www.ncbi.nlm.nih.gov/geo/) under accession numbers GSE85216, GSE85215, and GSE85214.

Address correspondence and reprint requests to Dr. Rocio T. Martinez-Nunez, King's College London, Guy's Campus, Guy's Hospital, 5th Floor Tower Wing, London SE19RT, U.K. E-mail address: rocio.martinez_nunez@kcl.ac.uk

The online version of this article contains supplemental material.

Abbreviations used in this article: AS, alternative splicing; BEC, bronchial epithelial cell; DBG, differentially bound gene; DBI, differentially bound isoform; DEG, differentially expressed gene; DEI, differentially expressed isoform; FDR, false discovery rate; Frac-seq, subcellular fractionation and RNA-seq; HC, healthy control; ID, identifier; IPA, Ingenuity Pathway Analysis; MRE, microRNA responsive element; Polysome, polyribosome-bound mRNA; qPCR, quantitative PCR; REC, research ethics committee; RNA-seq, RNA sequencing; RPM, read per million; SA, severe asthma; Total, cytoplasmic mRNA; UTR, untranslated region.

Copyright © 2018 by The American Association of Immunologists, Inc. 0022-1767/18/$35.00

Downloaded from http://www.jimmunol.org/ by guest on May 24, 2018

probable that additional mechanisms or steroid-unresponsive processes contribute to the disease persistence. As the airway epithelium orchestrates both inflammatory and remodeling processes relevant to SA (10, 11), we have focused on investigating alterations in this cell population. Moreover, we have centered on investigating posttranscriptional control of gene expression in asthma given that posttranscriptional control is considered key in the regulation of inflammation (12) and requires further understanding in many diseases, including asthma.

Popular approaches to studying complex diseases using high-throughput methodologies focus on the transcriptome, measured with arrays and sequencing technologies. However, it is appreciated that gene transcription and gene translation are not synonymous. From transcription to translation into protein, mRNA undergoes multiple processes, including splicing, stabilization, targeting by microRNAs, and decay (13), which affect mRNA loading into polyribosomes and subsequent translation. It is well acknowledged that the transcriptome shows weak correlation with the corresponding protein levels, as has been noted in early work (14). More recent works (15–17) show that the weak correlation can be improved upon by a machine-learning approach integrating transcript levels, transcript stability, polyribosome binding, and other sequence-based proxies of translation rates. Thus, the disparity between mRNA and protein levels in a variety of systems reflects the relevance of posttranscriptional mRNA regulation, demonstrating that cytoplasmic mRNA expression inadequately reflects actual translation into protein (13, 18). This disparity is even more pronounced in mammalian cells because of mRNA splicing. Alternative splicing (AS) generates several mRNAs from one single gene, with virtually all genes undergoing splicing (19). Alternatively spliced mRNA isoforms show preferential binding to polyribosomes (20) and heavily influence protein levels (21). Together, these observations highlight the need for consideration of splicing and translation when performing genome-wide mRNA expression measurements.

Given that microRNAs may affect mRNA levels and/or their translation into protein, as well as their importance in asthma, we sought to determine the genome-wide relationship between microRNAs and their mRNA targets in human asthma in different subcellular compartments. To this end, we performed microRNA profiling using small RNA sequencing (RNA-seq) and integrated it with subcellular fractionation and RNA-seq (Frac-seq) (20) in BECs isolated from human clinical samples from healthy volunteers and well-characterized SA patients. Frac-seq combines subcellular fractionation and RNA-seq, measuring mRNA levels in both cytoplasm (all mRNAs, cytoplasmic mRNA [Total]) and polyribosome-bound mRNA (Polysome; undergoing translation) fractions (22), facilitating the study of posttranscriptional mRNA regulation on a genome-wide scale.

Our work presents for the first time, to our knowledge, evidence that global control of mRNA splicing and translation is at the center of a human disease and asthma pathophysiology. Our results show that microRNAs are predicted to preferentially target polyribosome-associated mRNAs in asthma, adding valuable knowledge to the long-standing debate about microRNA effects on their targets (2, 5, 23, 24). More strikingly, among the microRNAs detected as differentially expressed between health and asthma, our results show that ~50% of the changes in mRNA binding to polyribosomes is modulated by a small hub of only six microRNAs. These six microRNAs account for ~90% of all cellular microRNA targeting and recapitulate disease characteristics when modulated in cells from healthy donors. Our work highlights the relevance of studying microRNAs in their molecular and cellular context and demonstrates the feasibility and importance of studying posttranscriptional gene regulation in asthma, opening a novel path in the understanding of the asthmatic process and potentially other inflammatory pathologies.

Materials and Methods

Study volunteers and consent to participate

Nonsmoking volunteers aged 18–65 y were recruited from the Wessex Severe Asthma Cohort and age/sex matched with healthy controls (HCs) from a departmental database (Supplemental Table I). All participants gave written informed consent. Adults with no history of respiratory disease, no current symptoms, and who did not achieve a 20% drop in forced expiratory volume in one second with inhaled methacholine at 16 mg/ml were defined as HCs. SA patients had inadequately controlled disease, (Asthma Control Questionnaire score of ≥1.5), despite management at Step 4/5 of the British Thoracic Society/Scottish Intercollegiate Guidelines Network asthma guidelines (four at step 5) and fulfilled the European Respiratory Society/American Thoracic Society criteria for SA. The study had prior ethics approval from the Southampton and South West Hampshire local research ethics committee (REC; REC reference number 05/Q1702/165). BECs used in the microRNA transfection experiments also had ethical approval (REC reference number 06/Q0505/12).

Spirometry, bronchoscopy, and cell culture

Spirometry was performed using the JAEGER MasterScreen with Viasys software. Measures were made before and 15 min after the administration of nebulized salbutamol (2.5 mg).

Flexible bronchoscopy was undertaken as previously described (25) according to British Thoracic Society guidelines and the local departmental standard operating procedure in the National Institutes for Health Research Respiratory Bioscience Research Unit, which is part of the Southampton Centre for Biomedical Research at Southampton General Hospital (Southampton, U.K.). Four separate sets of epithelial brushings were obtained from the right bronchus intermedius using disposable, sheathed bronchial brushes (BC-202D-1210; Olympus). Brushings were spun in plain RPMI 1640 and supplemented with penicillin/streptomycin (Thermo Fisher Scientific, Loughborough, U.K.) at 1200 rpm for 10 min. The medium was discarded, and cells were resuspended in complete BEC growth medium (Lonza, Blackley, U.K.). BECs were cultured as previously described (7). Briefly, BECs were cultured in collagen-coated (Thermo Fisher Scientific) T25 flasks in BEC growth complete medium (Lonza) and passaged onto 15 cm^2 dishes when 80% confluent. All expression experiments were done in passage 1 cells. BECs employed in the microRNA transfection experiments were isolated as in Crowley et al. (26) and were of passages 3–4.

Small RNA-seq

Libraries and small RNA-seq were done in Ocean Ridge Biosciences (Deerfield Beach, FL). Libraries were made employing NEBNext Small RNA-Seq Library Preparation Kit (New England BioLabs, Ipswich, MA) according to manufacturer's instructions and purified using a gel-based extraction method. The quality and size distribution of the amplified libraries were determined using an Agilent 2100 High Sensitivity DNA Bioanalyzer microfluidic chip. Libraries were quantified using the KAPA Library Quantification Kit (KK4824; Kapa Biosystems, Boston, MA). Libraries were pooled at equimolar concentrations and diluted prior to loading onto the flow cell of the cBot cluster station (Illumina, San Diego, CA). Libraries were extended and bridge amplified to create single-sequence clusters using the TruSeq Rapid SR Cluster Kit – HS. Ten percent ΦX174 phage DNA was spiked in all sequencing lanes for sequencer calibration. Real-time image analysis and base calling were performed on the instrument using the HiSeq Sequencing Control Software version 2.0.12.0 (Illumina). Libraries were sequenced with 50 bp single-end reads plus index read (TruSeq Rapid SBS Kit- HS 200 Cycle; Illumina). An average of 4.6 M reads passing trimming and minimum count filter (≥5 reads) was generated per sample.

CASAVA software version 1.8.4 was used for demultiplexing, removal of low quality reads, and production of FASTQ sequence files. The FASTX (http://hannonlab.cshl.edu/fastx_toolkit/index.html) application was used to trim the 3′ end of sequence reads to remove the 3′ adaptor sequence. Sequences without any 3′ adapter sequence, as well as sequences of <17 nucleotides after trimming, were removed. A perl script was used to remove sequences with any amount of 5′ adapter sequence. FASTX was also used to collapse identical reads into single entries retaining the read count for each unique sequence. Alignment results files were parsed by a custom perl script to generate FASTA files containing the read count and

Downloaded from http://www.jimmunol.org/ by guest on May 24, 2018

annotation for each unique sequence. An additional perl script was used to parse the annotated FASTA to determine the raw sequence read count for each target database entry in each sample; these counts were written to tabular format text files. To filter out any sequencing errors, only sequence reads that occurred ≥5 were retained for further analysis. Nonredundant sequences were then aligned to genomic (hg19) and mRNA sequence (hg19) using bowtie2 (27); sequences with perfect match and 1 nt mismatch (to aid mapping) were retained for further analysis. The genome-mapped sequences were further aligned to precursor and mature microRNAs in miRBase 21.0 (28) using OMAP# alignment software developed at Ocean Ridge Biosciences. To facilitate statistical analysis, the raw reads were converted to reads per million (RPM) (genome) mapped reads. Only sequences with a perfect match were retained for statistical analysis. Mature microRNA RPM values were normalized using the following formula: raw count/perfectly matched microRNA reads × 1,000,000. Tables were filtered to retain a list of annotated RNAs having a minimum of 10 mapped reads (detection threshold) in 25% of samples; for these filtered read tables, missing values were replaced with the average RPM value equivalent to one read. Library packages are available on CRAN. The principal component analysis plot in Fig. 1 was done employing Qlucore Omics Explorer. MicroRNA clustering in Fig. 1 was done in R using kendall/ward.D method.

Polyribosome profiling

Polyribosome profiling was done as described previously (20, 22), with the addition of 500 μg/ml cycloheximide (Sigma-Aldrich, Dorset, U.K.) in the lysis buffer, in passage 1 BECs. Briefly, cytoplasmic extracts were spun at 8000 rpm at 4°C in a minifuge. Supernatants were carefully removed, and 10% was saved for cytoplasmic (Total) RNA extraction; the rest was carefully loaded onto sucrose gradients. Preparation of the gradients, reading of polyribosome profiles, and extraction of individual polyribosome peaks were all done employing a Gradient Station (BioComp Instruments, Fredericton, NB, Canada) equipped with Bioprobes. Polyribosome profiles were generated reading the absorbance at 260 nm of spun gradients immediately after ultracentrifugation. The 80S-to-polyribosome ratio is a signature of the translational status of cells, and it is greatly modified when global translation is increased or impaired (29). We did not observe a difference in the translational profile between HCs and SA, as shown by similar ratios of monosome (80S) to polyribosome peaks (Fig. 3B, Supplemental Fig. 1). Polysome excludes the monosomal fraction (80S) as this may contain mRNAs not undergoing translation or lowly expressed genes (29, 30). RNA was isolated from the individual polyribosomal peaks (as well as total RNA) employing TRizol LS (Sigma-Aldrich) following manufacturer's instructions and was pooled to constitute the Polysome fraction and sequenced.

RNA-seq

RNA quality was assessed using a Bioanalyzer (Agilent) with all sequenced samples showing an RNA integrity number value >7 (RNA integrity number average ± SD = 8.95 ± 0.62). Libraries and sequencing were done in Expression Analysis (Durham, NC). Libraries were made using TruSeq Stranded mRNA Library Prep Kit (Illumina) and sequenced in a Hiseq 2500 (Illumina) platform (100 bp, paired-end sequencing). A minimum of 14 M reads per sample was generated. Upon completion of sequencing, base call files were converted into FASTQ files using Illumina Software (CASAVA). To prepare the reads for alignment, the sequencing adapters and other low-quality bases were clipped. Reads were aligned to External RNA Controls Consortium sequences to assess the success of library construction and sequencing. A subset (~1 M reads) was aligned to other spiked-in control sequences (PhiX and other Illumina controls used during library preparation), residual sequences (globin and rRNA), and poly-A/T sequences that persisted after clipping. The reads were also aligned to a sampling of intergenic regions to assess the level of DNA contamination. To determine the origin of all reads as a method of quality control, the unaligned reads were aligned to the full genome (not transcriptome) using Burrows–Wheeler Aligner 0.6.2 (31). RSEM v1.2.0 was used to quantify and compute estimated counts by genes and transcripts (32) using the University of California, Santa Cruz Genome Browser knownGene. All 77,000 isoforms defined by the University of California, Santa Cruz Genome Browser hg19 were considered as initial candidates; 12,485 isoforms are associated with only one gene, and thus were not considered further. Over 12,000 isoforms had 0 or nearly 0 counts for all subjects. Upper quartile normalization was used to normalize between different samples with different read depths for both aggregate gene expression and isoform analysis. Each sample was scaled so that the upper quartile of counts was equal to 1000. Only genes and isoforms with median counts of 10 or more on each group (Total or Polysome) were taken into account. PROC-GLM was used to perform preliminary statistical analysis (code at https://gist.github.com/rociotmartinez/7284e38817fe3ba09aca515c4f845bdb). Clustering methods employed were in heatmaps for differentially expressed genes (DEGs; Figs. 2, 3) using the Pearson/McQuitty method and in heatmaps for differentially expressed isoforms (DEIs; Figs. 4, 5) using the Kendall/centroid method. Heatmaps and generation of z-scores (which scales values according to mean and SD) were done in R.

Reverse transcription, quantitative PCR, and splicing assays

MicroRNA validations were performed using the miScript system (Qiagen, Manchester, U.K.) following manufacturer's instructions. MicroRNA expression was normalized against hsa-let-7a-5p.

RNA was reverse transcribed using the High Capacity cDNA Reverse Transcription Kit (Thermo Fisher Scientific). Validations for DEGs in Total and Polysome and microRNA effects (Figs. 2–6) were performed employing quantitative PCRs (qPCRs) using TaqMan Gene Expression Assays (Thermo Fisher Scientific) and using the primers with maximum coverage. *EGFR* primers in Supplemental Fig. 8 were kindly provided by N. Smithers and designed by Dr. D. Smart (both at the University of Southampton, Southampton, U.K.) and used as a SYBR Green assay (GoTaq qPCR Master Mix; Promega, U.K.). Primers employed for splicing assays in Figs. 4 and 5 were as follows: ACBD4_FOR: 5′-TGAATGGAGATGTTGGGGCT-3′; ACBD4_REV: 5′-TAGTGCTCGAACTGTCCCCA-3′; IRAK3_FOR: 5′-CACACGCTGCTGTTCGAC-3′; IRAK3_REV: 5′-TATATTTGGAAATCCACCTTCCTG-3′; ITGA2_FOR: 5′-CTGGTGTTAGCGCTCAGTCA-3′; ITGA2_REV: 5′-GTTCCTGGTGAGGATCAAGC-3′; ITGA6_FOR: 5′-GTGTTTATACTATGGAAGTGTGG-3′; ITGA6_REV: 5′-CGTTCCACTTTGTGATCCACT-3′. Primers employed in Supplemental Fig. 8 for *EGFR* detection were as follows: EGFR FOR: 5′-GGAGAACTGCCAGAAACTGACC-3′, EGFR REV: 5′-GCCTGCAGCACACTGGTTG-3′.

Gene expression was normalized against *GAPDH*. Splicing was measured employing a Bioanalyzer 2100 (Agilent), and the percentage spliced was calculated as Included/(Included + Skipped).

Pathway analysis

Data were analyzed using QIAGEN's Ingenuity Pathway Analysis (IPA; QIAGEN, www.qiagen.com/ingenuity), employing genes/isoforms with a cut-off of $p \leq 0.05$ [Benjamini–Hochberg adjusted $p \leq 0.05$ (33)]. Analysis with a cut-off of $p \leq 0.01$ missed important disease-related information. Grouping of pathways was done employing the IPA database and bibliography.

MicroRNA analysis

MicroRNA::target interaction in Fig. 6 was determined by cross-referencing the upregulated DEIs and DBIs (as gene identifier [ID]) with the downregulated microRNAs and vice versa, employing TargetScan 7.1 (34). We increased the stringency by accounting only for isoform ratios (SA/HC) of >1.5 or <0.66. Importantly, when sliding the ratios to <0.5 or >2 as well as not adding any restrictions on ratios, our results relating to the mRNA expression cumulative distributions differences remained significant (Supplemental Fig. 4). Interactive networks in Supplemental Interactive Figs. 1 and 2 were done employing networkD3 package in R.

MicroRNA transfections

MicroRNA transfections were performed using INTERFERin (Polyplus Transfection, Illkirch, France) following manufacturer's instructions as in Martinez-Nunez et al. (7). Briefly, 16 nM of each anti- or pre-microRNA were transfected into BECs from HCs. Forty-eight hours posttransfection, cells were preincubated or not with 10^{-7} M dexamethasone during 2 h and stimulated with 10 ng/ml IL-1β (or vehicle). Cells were harvested 24 h after stimulation, and RNA was extracted and analyzed.

Image processing

Graphs for polyribosome profiles, validations, pathway analyses, and microRNA analyses were produced using GraphPad Prism versions 6.07 or 7 (GraphPad Software, San Diego, CA, www.graphpad.com). Heatmaps were produced using R statistical language, version 3.2.0 (R project for Statistical Computing, https://www.r-project.org/), and their labels were clarified in Adobe Illustrator CS5. All packages used in R are available in the CRAN repository. All figures panels were put together using Adobe Illustrator CS5. Frequency distribution plots in Supplemental Fig. 4 were done by adjusting the data to a nonlinear regression to facilitate and clarify data presentation employing GraphPad Prism v6.07.

Statistical analysis

Clinical parameters statistics (except for sex and atopy) as well as statistical analyses of validations were done employing a Mann–Whitney *U* test for

Downloaded from http://www.jimmunol.org/ by guest on May 24, 2018

nonparametric data and unpaired t tests for parametric data comparisons, according to D'Agostino & Pearson omnibus normality test. Differences in sex and atopy between HC and SA were tested employing a Fisher exact test. Statistical analysis was performed using GraphPad Prism version 6.07 or 7.

MicroRNAs shown in Fig. 1A and 1B had a $p \leq 0.05$ and a restricted fold change of <0.66 or >1.5 (SA/HC), which showed a false discovery rate (FDR) ≤0.05 when corrected using the Benjamini–Hochberg method (33). For gene and isoform expression, a restrictive $p \leq 0.01$ (two-group t test) was taken to perform the heatmaps in Figs. 2–5. Nominal significant p values from RNA-seq datasets (two-group test, $p \leq 0.01$ and $p \leq 0.05$, Supplemental Datasets 1, 3, 5, 7) were corrected by applying the Benjamini–Hochberg method (33) employing R, which showed an FDR ≤ 0.05 for all genes and isoforms displayed in Figs. 2–5 and used in pathway analysis. FDR was calculated experimentally also, based on the gene expression assays (0.136) and was in the 0.1–0.2 range in accordance with previous studies (20, 35). The p value displayed in all pathway analyses was calculated in IPA employing a Fisher exact test.

Statistical analysis of proportions for microRNA targeting between Total and Polysome (Fig. 6) was done employing the Fisher exact test in GraphPad Prism version 6.07. Statistics comparing cumulative distributions in Supplemental Fig. 4 were performed employing a Kolmogorov–Smirnov test as in Agarwal et al. (34) using GraphPad Prism v6.07.

The sequencing datasets used for analysis have been deposited and are publicly available in the National Center for Biotechnology Information Gene Expression Omnibus repository (http://www.ncbi.nlm.nih.gov/geo/) under accession numbers GSE85216, GSE85215, and GSE85214.

Results

SA BECs present genome-wide differences in microRNA levels compared with healthy donors

To determine microRNA expression, we performed small RNA-seq on BECs (HC = 5; SA = 8). The demographics of the study population are in Supplemental Table I, highlighting the main clinical characteristics that differed between healthy controls and severe asthmatic patients. Lung function and cellular profile of their bronchoalveolar lavage was found statistically significant between health and SA, as expected. There were no statistically significant differences in age, sex, atopy, or weight (body mass index) between the two groups. HCs had no history of respiratory disease or current symptoms and no evidence of abnormal bronchial reactivity on methacholine inhalation challenge testing. SA patients had inadequately controlled disease and fulfilled the European Respiratory Society/American Thoracic Society criteria for SA. Principal component analysis (employing microRNAs with a $p < 0.05$ between HC and SA, $0.66 >$ SA/HC ratio > 1.5, Supplemental Table II) identified that widespread microRNA expression is different between HC and SA patients. Unsupervised hierarchical clustering of 21 differentially expressed microRNAs separated the samples between health and disease, with the exception of SA3 (Fig. 1B). We validated these findings with microRNA qPCRs on an expanded cohort (n = 9 HC and n = 11 SA, Fig. 1C, most differentially expressed microRNAs). MicroRNAs -19b-3p, -20a-5p, 135b-5p, -574-3p, and 625-3p were validated, whereas only miR-127-3p showed no significant differences between SA and HC among the candidates tested.

IPA highlighted the impact of the remaining 20 dysregulated microRNAs on molecular and cellular functions of relevance to asthma (Supplemental Table III), as well as association with "Organismal Repair and Abnormalities" (18 microRNAs), "Inflammatory Response," and "Immunological Disease" (nine microRNAs each). Thus, microRNAs dysregulated in SA may underlie important general pathological processes in asthma related to epithelial repair and inflammation via posttranscriptional mRNA regulation.

Total mRNA expression is altered in SA bronchial epithelium

As microRNAs may regulate mRNA levels by destabilization (4, 24), we performed transcriptomics analysis by RNA-seq. Genome-wide mRNA expression analysis revealed 16,277 expressed genes in BECs (median read counts ≥10) with 194 DEGs ($p \leq 0.01$, Supplemental Dataset 1). Unsupervised cluster analysis of DEGs separated HC and SA samples (Fig. 2A). qPCRs (Fig. 2B, Supplemental Fig. 2) validated a decreased expression of *COL21A1*, *CEBPA,* and *CTSD* mRNAs and an upregulation of *IGFL1*, *IL23A*, *ABCC4*, *PDPN,* and *IL31RA* gene expression in SA compared with HC on an expanded cohort (n = 10 HC, n = 11 SA).

IPA identified dysregulated pathways attributable to the detected DEGs (Fig. 2C, Supplemental Dataset 2). This revealed non–type 2 inflammatory pathways, as well as glucocorticoid activation–-and drug metabolism-related pathways. The pathway with the strongest statistically significant dysregulation (p = 0.001) was PXR/RXR (pregnane X receptor/retinoid X receptor), related to endobiotic and xenobiotic/drug metabolism (36), consistent with the high-dose corticosteroid therapy prescribed to the severe asthmatics (37). Dysregulated LPS/IL-1 mediated inhibition of RXR function (p = 0.0055) and 1,25-dihydroxyvitamin D3 biosynthesis (p = 0.0049) were also evident.

Translation in SA bronchial epithelium is altered at the genome-wide level

Frac-seq was performed to determine the levels of mRNAs undergoing translation in BECs (Fig. 3A) in the same healthy individuals and SA patients as in Figs. 1 and 2. Fig. 3B depicts two representative polyribosome profiles of both HCs and SA patients (remaining in Supplemental Fig. 1). The same mRNAs as previously detected (Fig. 2) were evident in the Polysome fraction (16,277 genes, median read counts ≥ 10). SA patients and healthy donors differed in the binding to polyribosomes for 243 genes (differentially bound genes [DBGs], $p \leq 0.01$, Supplemental Dataset 3). Unsupervised hierarchical clustering of DBGs distinguished between HC and SA (Fig. 3C). Of note, SA patients with earlier-onset disease (onset <25 y old) clustered differently to the other five SA samples (onset >40 y old). Fig. 3D and Supplemental Fig. 3 show the results from the validations of several candidate genes on the expanded cohort employing qPCRs (n = 10 HC, n = 11 SA). This confirmed that *IGFL1*, *IL23A*, *IL1A*, *PDPN*, *IL31RA*, *ABCC4,* and *LTB* genes were all more bound to polyribosomes in SA than in HC. In contrast to total mRNA, there was no evidence of decreased polyribosomal binding of *COL21A1* in SA.

Pathway analysis was undertaken, and dysregulated pathways were clustered into the same categories as in Fig. 2C (Fig. 3E, Supplemental Dataset 4). Unlike DEGs in Total, DBGs in Polysome did not map to glucocorticoid or endobiotic metabolism. Pathways present in Polysome DBGs and absent in Total DEGs included TLR signaling (p = 0.04) and IL-1–related inflammation (p = 0.004), both implicated in SA (38, 39), as well as phagosome formation (p = 0.025).

Together, these results identify that there is genome-wide dysregulation of translation (mRNAs bound to polyribosomes) in asthma and that this impacts additional pathways and genes that differ from those detected when analyzing total mRNA levels, suggestive of an underlying strong posttranscriptional signature.

Isoform mRNA analysis reveals structural and inflammatory anomalies in SA bronchial epithelium not disclosed by aggregate gene expression

AS analysis of the RNA-seq data revealed 30,831 mRNAs (median counts ≥10) in both Total and Polysome fractions. Differential expression analysis of isoforms (DEIs; $p \leq 0.01$, Supplemental Dataset 5) revealed 319 mRNA isoforms differentially expressed

Downloaded from http://www.jimmunol.org/ by guest on May 24, 2018

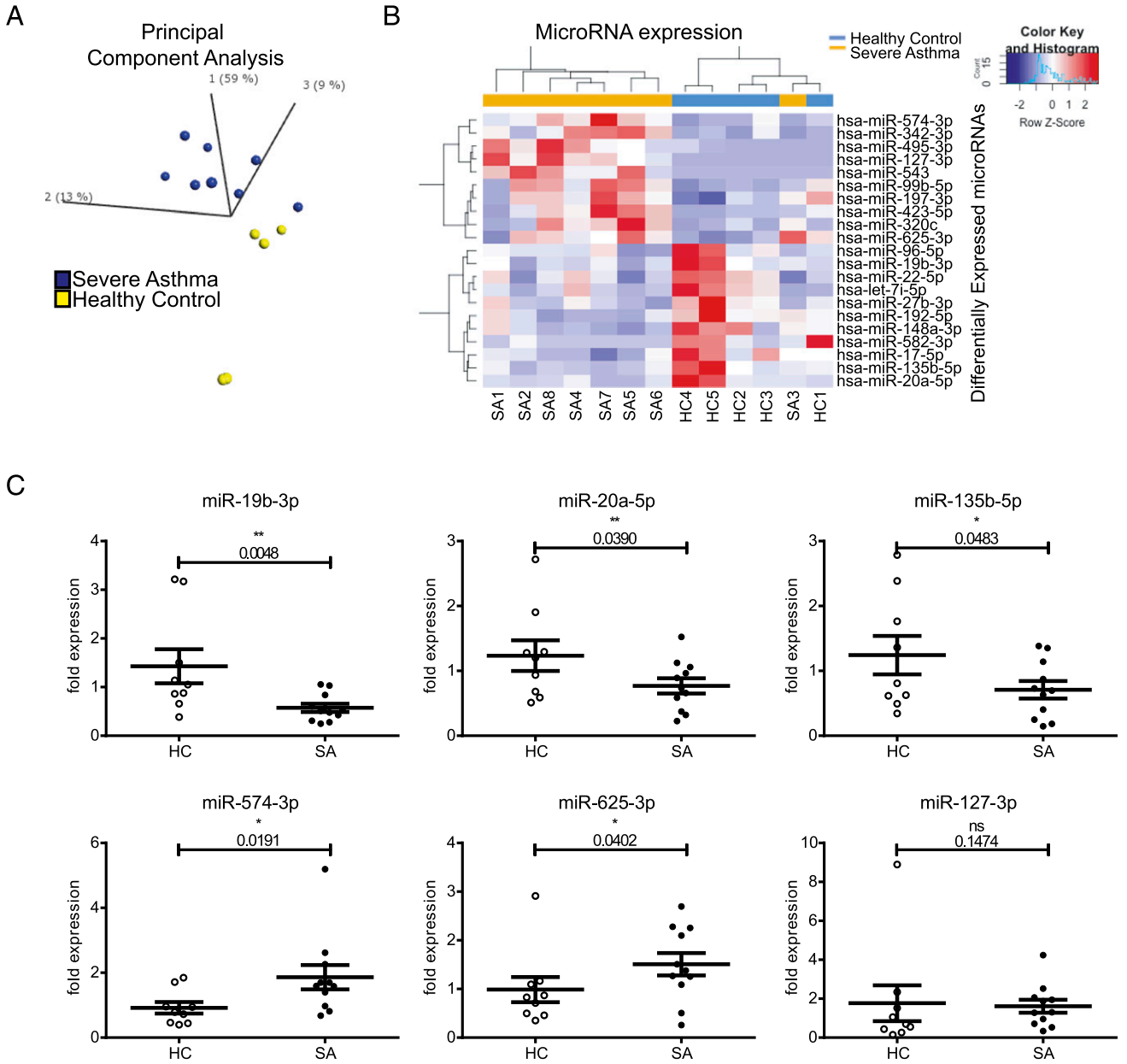

FIGURE 1. MicroRNAs are dysregulated in human SA bronchial epithelium. (**A**) Principal component analysis plot showing the distribution of healthy (yellow) and SA (blue) samples, according to the levels of differentially expressed microRNAs (microRNAs with a $p < 0.05$, $0.66 >$ SA/HC ratio > 1.5). (**B**) Heatmap depicting unsupervised clustering of HCs and severe asthmatics based on the expression values of differentially expressed microRNAs ($p < 0.05$, $0.66 >$ SA/HC ratio > 1.5). (**C**) Dot plots (mean + SEM) representing qPCR analysis of several microRNAs ($n = 9$ HC, $n = 11$ SA). Statistics were done employing t tests. $*p < 0.05$, $**p < 0.01$.

between HC and SA in Total. Unsupervised clustering of DEIs clearly distinguished healthy and SA samples (Fig. 4A), indicating that the bronchial epithelial expression of alternatively spliced mRNAs is different globally between HC and SA.

The DEIs mapped to genes that were detected as differentially expressed in Total genes (Fig. 2, overlap of ~32% DEIs gene IDs in DEGs at $p < 0.01$), although AS analysis also revealed new candidates validated employing splicing assays. Fig. 4B depicts the results: the left column shows the results from AS assays (RT-PCRs quantified using a Bioanalyzer), and the right column shows those of aggregate gene expression (i.e., all isoforms, measured by qPCRs). The skipped isoform of *IRAK3* (IL-1 receptor–associated kinase 3) was increased in SA BECs but was not detected differentially expressed employing aggregate gene expression assays. In contrast, aggregate gene expression analysis detected *ACBD4* as downregulated in SA, whereas AS analysis revealed no difference. Thus, AS analysis reveals novel candidates related to asthma biology involved in inflammatory functions of bronchial epithelium not disclosed by aggregate gene expression analysis.

DEIs were mapped onto pathways using IPA and grouped similarly to Figs. 2 and 3 with the addition of epithelial repair/remodeling pathways (Supplemental Dataset 6), which became apparent when performing AS analysis. Fig. 4C shows six pathways among the top 10 according to p value. Consistently with our previous findings in Total DEGs (Fig. 2C), Total DEIs affected glucocorticoid signaling ($p = 0.0044$), but analysis of isoforms detected new pathways, including IL-6–JAK/STAT signaling ($p = 0.004$).

To interrogate the impact of AS on mRNA translation, we also analyzed alternatively spliced isoforms on polyribosome-bound

Downloaded from http://www.jimmunol.org/ by guest on May 24, 2018

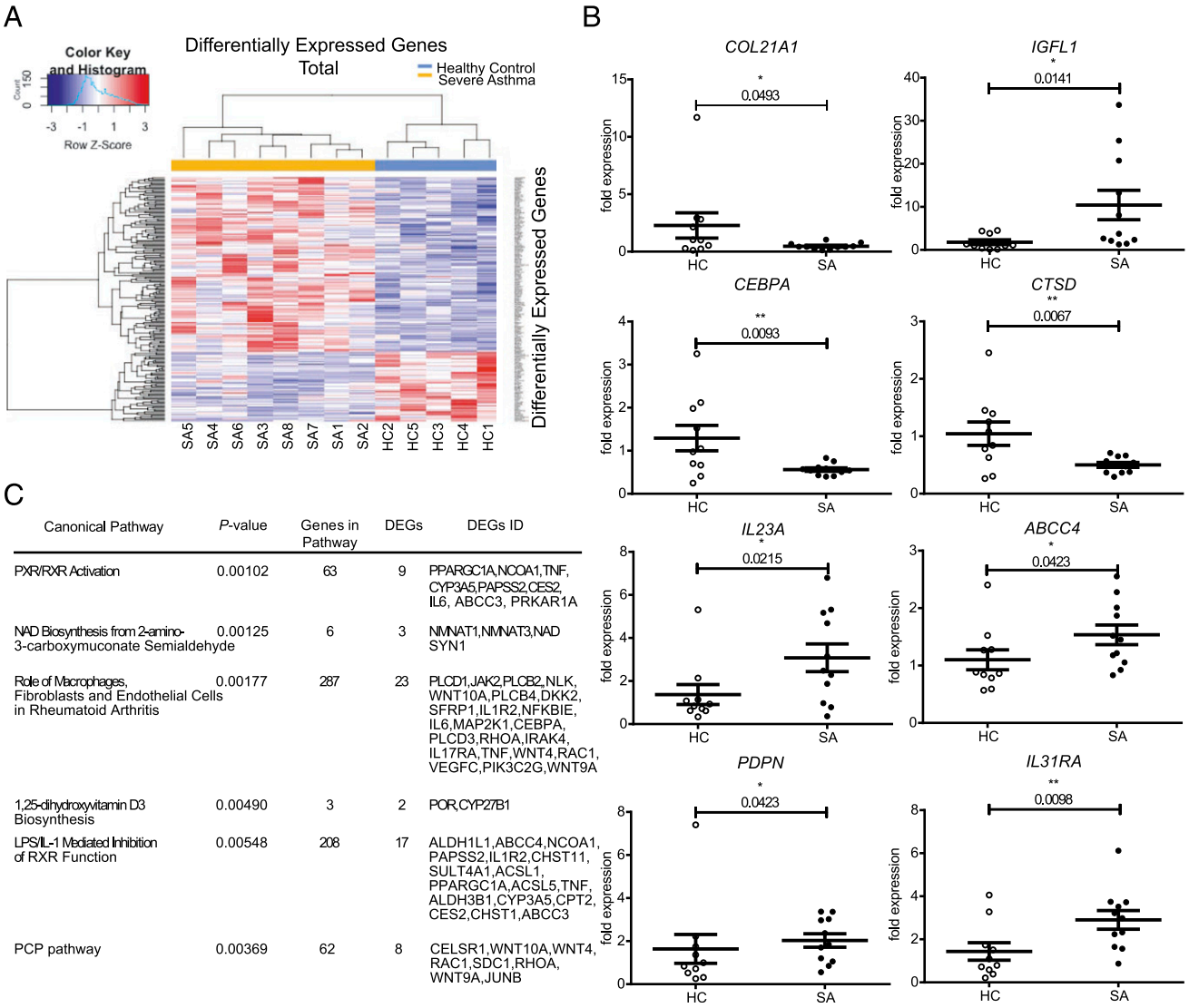

C

Canonical Pathway	*P*-value	Genes in Pathway	DEGs	DEGs ID
PXR/RXR Activation	0.00102	63	9	PPARGC1A,NCOA1,TNF, CYP3A5,PAPSS2,CES2, IL6, ABCC3, PRKAR1A
NAD Biosynthesis from 2-amino-3-carboxymuconate Semialdehyde	0.00125	6	3	NMNAT1,NMNAT3,NAD SYN1
Role of Macrophages, Fibroblasts and Endothelial Cells in Rheumatoid Arthritis	0.00177	287	23	PLCD1,JAK2,PLCB2,NLK, WNT10A,PLCB4,DKK2, SFRP1,IL1R2,NFKBIE, IL6,MAP2K1,CEBPA, PLCD3,RHOA,IRAK4, IL17RA,TNF,WNT4,RAC1, VEGFC,PIK3C2G,WNT9A
1,25-dihydroxyvitamin D3 Biosynthesis	0.00490	3	2	POR,CYP27B1
LPS/IL-1 Mediated Inhibition of RXR Function	0.00548	208	17	ALDH1L1,ABCC4,NCOA1, PAPSS2,IL1R2,CHST11, SULT4A1,ACSL1, PPARGC1A,ACSL5,TNF, ALDH3B1,CYP3A5,CPT2, CES2,CHST1,ABCC3
PCP pathway	0.00369	62	8	CELSR1,WNT10A,WNT4, RAC1,SDC1,RHOA, WNT9A,JUNB

FIGURE 2. Genome-wide mRNA expression is dysregulated in SA. (**A**) Heatmap showing unsupervised clustering of DEGs ($p \leq 0.01$) in the Total fraction. (**B**) Dot plots (mean + SEM) representing qPCRs validating the RNA-seq dataset (n = 10 HC, n = 11 SA). Statistics were done employing t tests. (**C**) Table showing 6 of the top 10 pathways predicted by IPA for DEGs. Statistics were done employing Fisher two-tailed test. $*p < 0.05$, $**p < 0.01$.

mRNAs. This identified 335 mRNA isoforms differentially bound to polyribosomes (differentially bound isoforms [DBIs]) between HC and SA (Supplemental Dataset 7) that allowed unsupervised clustering of the samples (Fig. 5A). Several candidates in the Polysome fraction were validated by splicing assays and possible differences with aggregate gene expression (overlap of ~37% DBIs gene IDs in DBGs at $p < 0.01$) assessed using qPCRs (Fig. 5B). The skipped isoforms of *ITGA2* and *ITGA6* genes presented increased polyribosome binding in SA, information that is missed when performing gene expression analysis. *ITGA6* and *ITGA2* encode for integrins, key structural proteins in cell adhesion, and signaling (40). *IRAK3* skipped isoform (increased only in Total DEIs, Fig. 4B) showed increased binding to polyribosomes when performing analysis of aggregate gene expression.

IPA of Polysome DBIs revealed downregulation of Notch signaling (Fig. 5C, Supplemental Dataset 8), suggesting a decreased airway type 2 response (41) in SA. DBIs in Polysome determined dysregulation of telomere extension, with telomere length in leukocytes previously related to asthma (42). Polysome DBIs also revealed pathways relating to epithelial cell repair/remodeling (e.g., Calpain protease or Paxillin signaling) consistent with the airways epithelium impairment observed in asthma (43).

Together, these data show that AS is dysregulated in SA bronchial epithelium at a global scale, affecting the translation of mRNAs encoding structural and inflammatory factors.

MicroRNAs associate with genome-wide changes in mRNA expression at the transcriptional and translational levels

To determine the genome-wide effect of microRNAs dysregulated in the bronchial epithelium of asthma patients, we aimed to identify which differentially expressed mRNAs were targeted by microRNAs on each fraction. To do so, we cross-referenced the predicted targets from TargetScan 7.1 (34) for the 20 microRNAs (Fig. 1, all except for miR-127-3p) with the DEIs in Total and Polysome (Figs. 4, 5), as microRNAs are known to target specific isoforms (44). This showed that microRNAs significantly modify the levels of both cytoplasmic and translating mRNAs (Supplemental Fig. 4). The overlap between targets in the cytoplasmic and Polysome fractions was very low (Fig. 6A, 11.2% of Total DEIs and 7.6% of Polysome DBIs), suggesting that microRNAs dysregulated in

Downloaded from http://www.jimmunol.org/ by guest on May 24, 2018

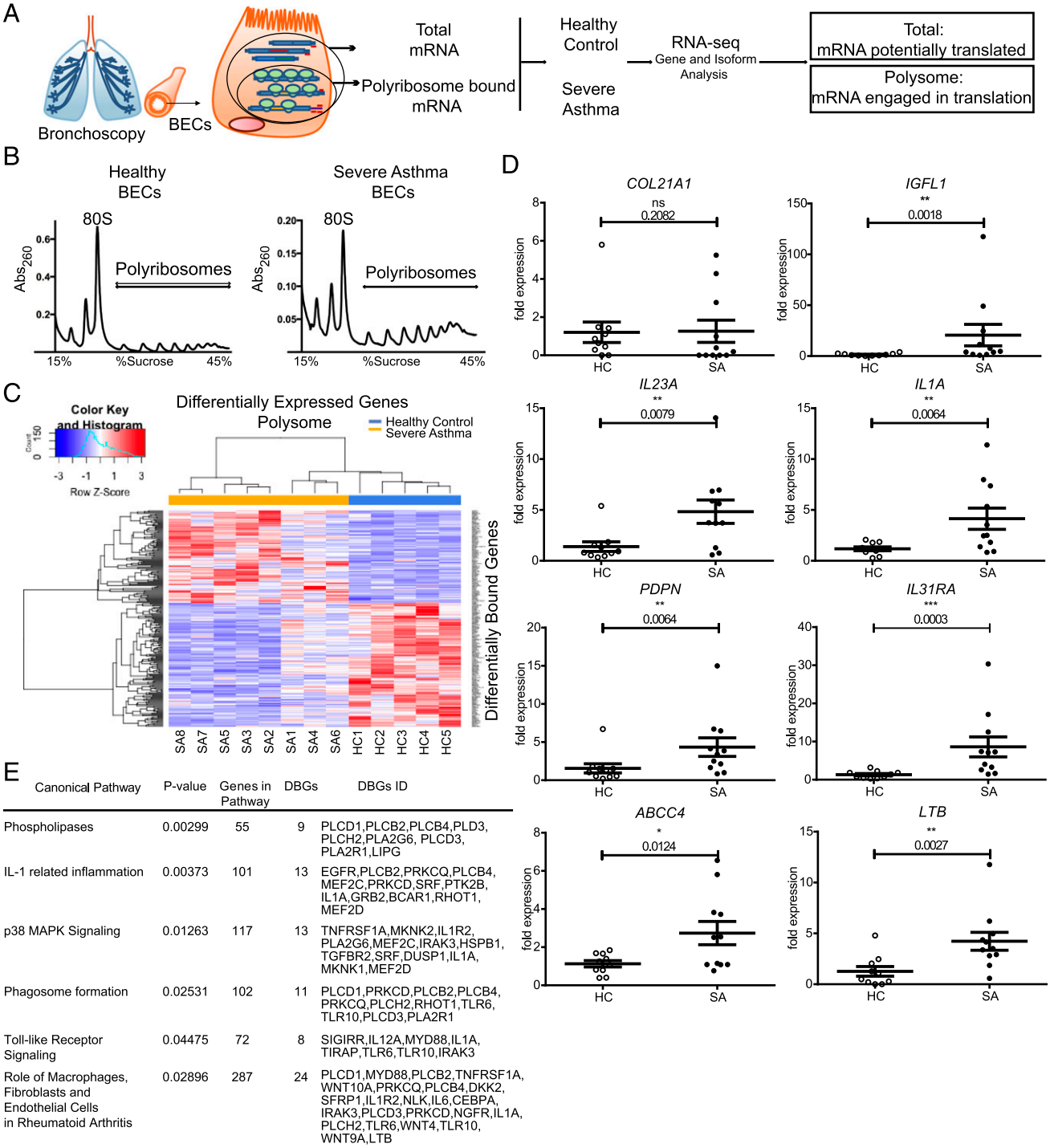

E

Canonical Pathway	P-value	Genes in Pathway	DBGs	DBGs ID
Phospholipases	0.00299	55	9	PLCD1,PLCB2,PLCB4,PLD3, PLCH2,PLA2G6, PLCD3, PLA2R1,LIPG
IL-1 related inflammation	0.00373	101	13	EGFR,PLCB2,PRKCQ,PLCB4, MEF2C,PRKCD,SRF,PTK2B, IL1A,GRB2,BCAR1,RHOT1, MEF2D
p38 MAPK Signaling	0.01263	117	13	TNFRSF1A,MKNK2,IL1R2, PLA2G6,MEF2C,IRAK3,HSPB1, TGFBR2,SRF,DUSP1,IL1A, MKNK1,MEF2D
Phagosome formation	0.02531	102	11	PLCD1,PRKCD,PLCB2,PLCB4, PRKCQ,PLCH2,RHOT1,TLR6, TLR10,PLCD3,PLA2R1
Toll-like Receptor Signaling	0.04475	72	8	SIGIRR,IL12A,MYD88,IL1A, TIRAP,TLR6,TLR10,IRAK3
Role of Macrophages, Fibroblasts and Endothelial Cells in Rheumatoid Arthritis	0.02896	287	24	PLCD1,MYD88,PLCB2,TNFRSF1A, WNT10A,PRKCQ,PLCB4,DKK2, SFRP1,IL1R2,NLK,IL6,CEBPA, IRAK3,PLCD3,PRKCD,NGFR,IL1A, PLCH2,TLR6,WNT4,TLR10, WNT9A,LTB

FIGURE 3. Genome-wide translation is dysregulated in SA. (**A**) Schematic of Frac-seq experiment. RNA-seq was performed on Total and Polysome mRNA; Total HC versus Total SA and Polysome HC versus Polysome SA datasets were then compared. (**B**) Representative polyribosome profiles from healthy (left) and SA (right) BECs. (**C**) Heatmap showing unsupervised clustering of DBGs ($p \leq 0.01$) in the Polysome fraction. (**D**) Dot plots (mean + SEM) representing qPCRs validating the RNA-seq dataset (n = 10 HC, n = 11 SA). Statistics were done employing t tests. (**E**) Table showing six pathways predicted by IPA for DBGs not found in the Total fraction. Statistics were done employing Fisher two-tailed test. $^{*}p < 0.05$, $^{**}p < 0.01$, $^{***}p < 0.001$.

asthma may have different effects depending on the mechanism of action (mRNA degradation or blocking of translation). MicroRNAs showed preferential targeting of polyribosome-bound mRNAs (172/288) compared with cytoplasmic mRNAs (116/231) (Supplemental Fig. 5A, two-tailed Fisher exact test $p = 0.0331$) consistent with mRNAs presenting more or less MREs according to their association with polyribosomes [Supplemental Fig. 5B (20)]. These results suggest that dysregulated microRNAs in asthma may have more impact in protein translation than on mRNA levels.

The relevance of each one of the 20 microRNAs in targeting Total and Polysome mRNAs was then evaluated. Fig. 6B shows the number of targets per microRNA, which revealed that a group of only eight microRNAs controls most of the mRNA changes detected in SA both at cytoplasmic and polyribosome binding levels. Among those eight microRNAs, dysregulated expression of six

Downloaded from http://www.jimmunol.org/ by guest on May 24, 2018

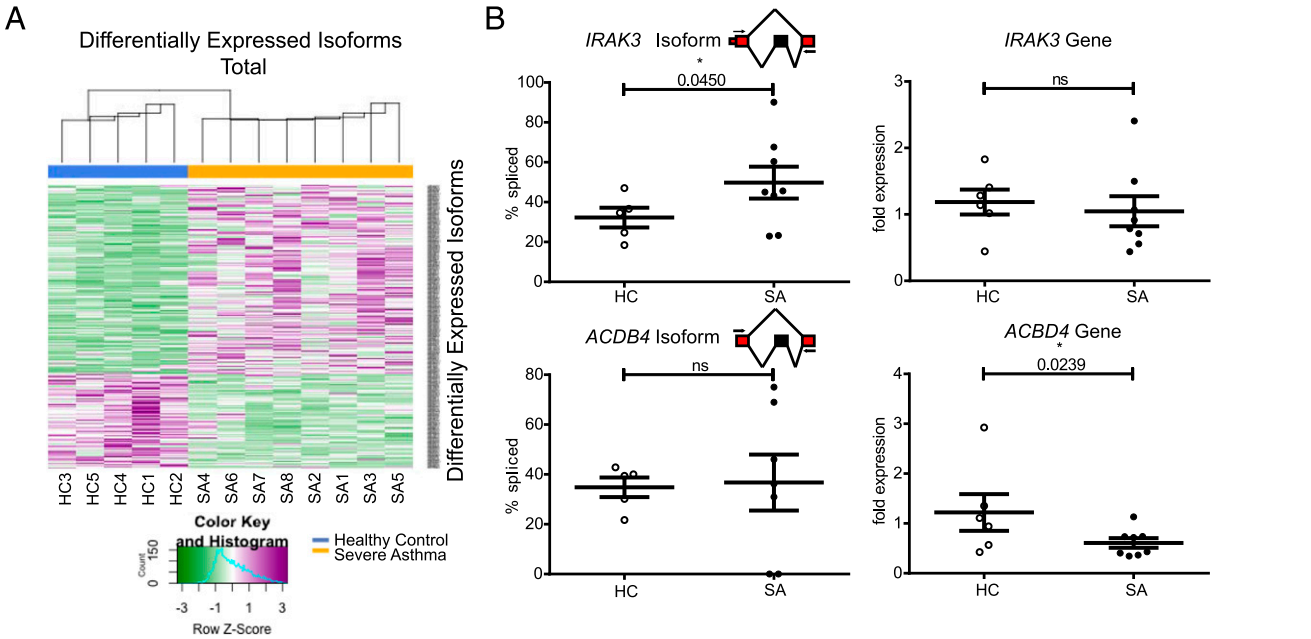

C

Canonical Pathway	*P*-value	Genes in Pathway	DEIs	DEIs Gene ID
Antioxidant Action of Vitamin C	0.00092	95	15	PLCD1,GLRX,JAK2,PLCB2,PLD3,MAPK12,PLCB4,NFKBIE,PLCD3,PLA2G4C,PNPLA3,TNF,STAT5A, PNPLA8,MAPK9
Role of Macrophages, Fibroblasts and Endothelial Cells in Rheumatoid Arthritis	0.00141	287	32	CSNK1A1,PLCB2,WNT10A,SMO,DKK2,CHP1,IL6R,CAMK2D,SFRP1,PDGFB,NFKBIE,IL6,MAP2K1,IRAK3, IL1RN,TNF,NFAT5,VEGFC,MAPK9,PLCD1,NFATC4,JAK2,RAF1,PLCB4,NLK,CEBPA,PLCD3,RHOA, IL17RA,CAMK2G,RAC1,WNT9A
Salvage Pathways of Pyrimidine Ribonucleotides	0.00174	91	14	NME7,CSNK1A1,DMPK,CDK7,AK9,CMPK1,MAP2K1,NME4,CDA,GRK5,UCK2,CMPK2,NME2,MAPK9
Cholecystokinin/Gastrin-mediated Signaling	0.00174	101	15	PLCB2,RAF1,MAPK12,PLCB4,RHOC,MAP2K1,PTK2,EPHA4,RHOA,IL1RN,TNF,BCAR1,RHOT1,MEF2B, MAPK9
Role of JAK family kinases in IL-6-type Cytokine Signaling	0.00404	25	6	JAK2,STAT5A,MAPK12,IL6R,IL6,MAPK9
Glucocorticoid Receptor Signaling	0.00440	272	29	HSPA1L,HSPA1A/HSPA1B,PLAU,CHP1,PRKAB1,NFKBIE,IL6,MAP2K1,PRKACB,IL1RN,TSC22D3,DUSP1, TNF,STAT5A,NFAT5,POMC,MAPK9,NFATC4,ERCC2,JAK2,CDK7,RAF1,MAPK12,BAG1,CEBPA,CREBZF, TGFBR2,UBE2I,RAC1

FIGURE 4. Genome-wide mRNA AS is dysregulated in SA and adds novel information to that detected by gene expression analysis. (**A**) Heatmap showing unsupervised clustering of donors according to DEIs ($p \leq 0.01$) in the Total fraction between HC and SA. (**B**) Dot plots (mean + SEM) representing the RT-PCR splicing assays for *IRAK3* and *ACBD4* skipped isoforms (HC $n = 5$, SA $n = 8$, left column) and their corresponding qPCR assay for aggregate gene expression (HC $n = 6$, SA $n = 8$, right column). RT-PCRs were quantified using an Agilent Bioanalyzer DNA microfluidic chip, and the percentage of splicing was calculated and plotted as % inclusion = [included isoform]/([included isoform]+[excluded isoform]). Statistics were done employing *t* tests. (**C**) Table showing six pathways predicted by IPA for DEIs in the Total fraction. Statistics were done employing Fisher two-tailed test. $^*p < 0.05$. ns, nonsignificant.

microRNAs was validated in our larger cohort of patients ($n = 11$ for each group, Fig. 6C, Supplemental Fig. 6). These six microRNAs were also predicted to preferentially modulate changes on translating mRNAs (48.2% as opposed to 35.9% in Total, Fig. 6D, $p = 0.0056$). Network analyses of microRNA target interactions showed that the target mRNAs of these six microRNAs are in many cases coregulated by multiple microRNAs. This suggests that the expression of these mRNAs is tightly controlled but disrupted in SA patients (interactive networks in Supplemental Interactive Figs. 1, 2, data in Supplemental Datasets 9, 10). Strikingly, this network of six microRNAs was predicted to control almost 90% of all targeted mRNAs in the Polysome fraction (Fig. 6E), which mapped to inositol pathways and cell cycle (Fig. 6F, Supplemental Table IV), the latter desynchronized in asthma (45).

To validate our findings, we transfected BECs from healthy donors with the microRNA network to evaluate the effects of the dysregulated microRNA hub found in SA BECs. Namely, anti–miR-22-5p, anti–miR-148a-3p, pre–miR-342-3p, pre–miR-495-3p, pre–miR-543, and pre–miR-197-3p oligonucleotides were cotransfected at equimolar concentrations and compared with BECs cotransfected with negative anti-microRNA and pre-microRNA controls at equimolar concentrations. Cells were then treated with IL-1β, which is found upregulated in SA (and highlighted in our pathway analysis), as well as assessed for glucocorticoid sensitivity. Fig. 6G–I show that the microRNA network was able to ablate the inhibition by glucocorticoids of IL-1β–driven IL-6 mRNA expression (Fig. 6I). The microRNA hub was also able to upregulate *TGFBR2* mRNA expression (Fig. 6H) as well as significantly increase IL-1β–driven *TNF* mRNA expression. These are all characteristics well defined in SA patients, highlighting the biological importance of microRNA dysregulation in SA bronchial epithelium.

Integrated together, our data demonstrate that there is widespread deregulation of posttranscriptional processes in human asthma. Our work shows that the dysregulation of a microRNA hub causes genome-wide dysfunction in the translation of mRNAs encoding structural and inflammatory factors in the bronchial epithelium of SA patients and demonstrates the value of integrating multiple omics datasets when investigating human biological processes.

Discussion

Our work integrating Frac-seq and small RNA-seq reveals that microRNAs, cytoplasmic mRNAs, and translating mRNAs are all

Downloaded from http://www.jimmunol.org/ by guest on May 24, 2018

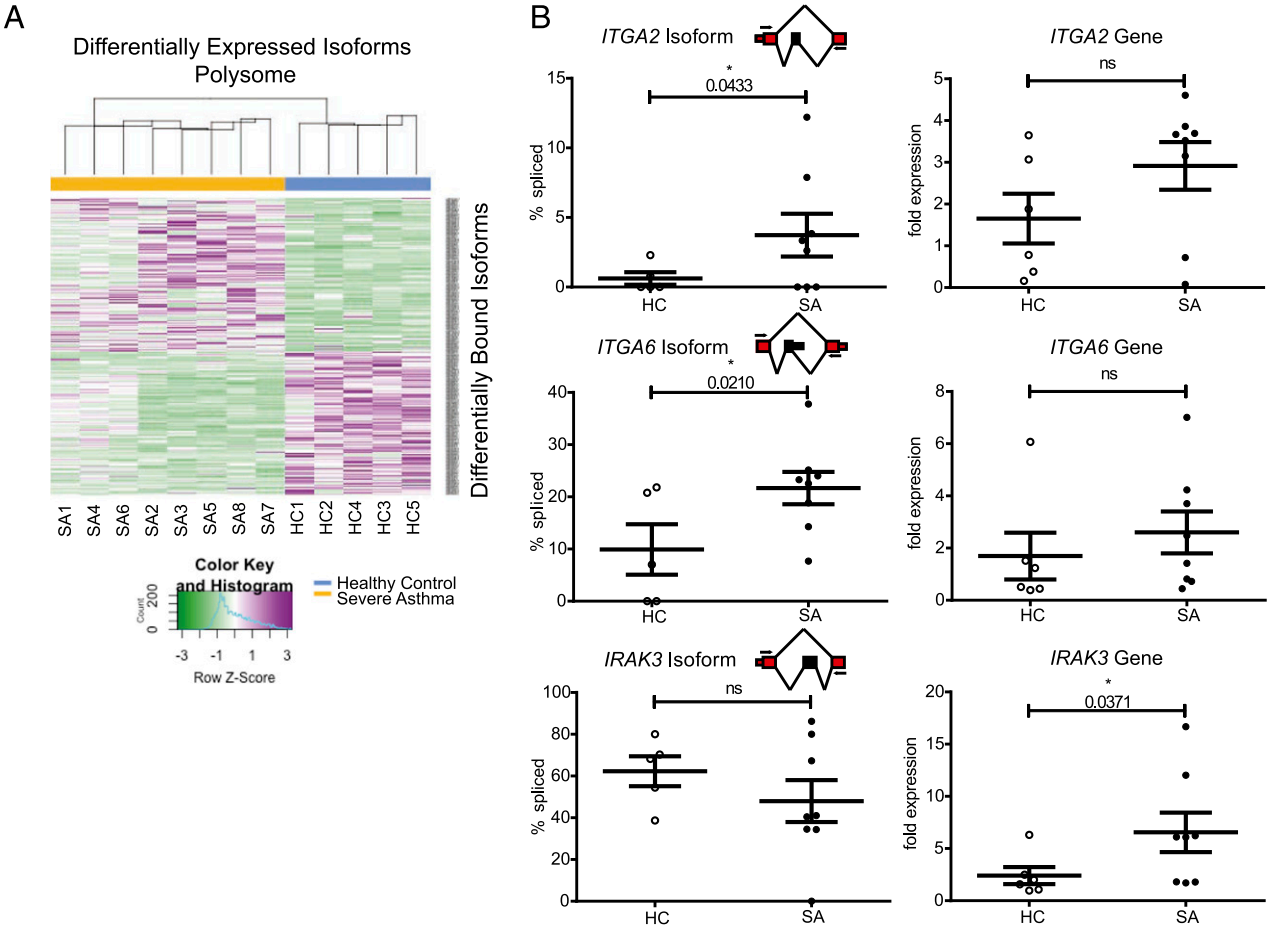

C

Canonical Pathway	*P*-value	Genes in Pathway	DBIs	DBIs Gene ID
Actin Nucleation by ARP-WASP Complex	0.00015	56	13	CDC42,RHOT2,RRAS2,ITGA2,VASP,PPP1R12C,ACTR3,ARPC2,BAIAP2,ARPC5,GRB2,RHOT1, FNBP1
Telomere Extension by Telomerase	0.00041	15	6	POT1,TERF2,TINF2,XRCC5,TNKS,NBN
Notch Signaling	0.00441	37	8	DLL1,PSEN2,MAML1,DTX2,JAG2,MAML3,NOTCH2,NUMBL
Regulation of Cellular Mechanics by Calpain Protease	0.01685	55	9	CCNA1,CNGB1,RRAS2,CCNE1,ITGA2,EZR,PXN,GRB2,TLN2
Paxillin Signaling	0.01117	98	14	JAK2,STAT5A,MAPK12,IL6R,IL6,MAPK9
ERK/MAPK Signaling	0.00861	186	23	PPP1CC,ATF2,RRAS2,ITGA2,PPP2R4,PPP1CA,PXN,MKNK2,PIK3C2B,TLN2,ELF3,ETS2, PPP1R3D,HSPB1,ELF5,SRF,DUSP1,PAK6,ELF4,GRB2,MKNK1,PRKAR1B,PRKACA

FIGURE 5. Genome-wide binding of mRNA isoforms to polyribosomes is dysregulated in SA, providing novel information to that detected by gene expression analysis. (**A**) Heatmap showing unsupervised clustering of donors according to DBIs ($p \leq 0.01$) in the Polysome fraction between HC and SA. (**B**) Dot plots (mean + SEM) representing the RT-PCR splicing assays for *ITGA2*, *ITGA6*, and *IRAK3* skipped isoforms (HC $n = 5$, SA $n = 8$, left column) and their corresponding qPCR results for aggregate gene expression (HC $n = 6$, SA $n = 8$, right column). RT-PCRs were quantified using an Agilent Bioanalyzer DNA microfluidic chip, and the percentage of splicing was calculated and plotted as % inclusion = [included isoform]/([included isoform] +[excluded isoform]). Statistics were done employing *t* tests. (**C**) Table showing six pathways predicted by IPA for DBIs not found in the Total fraction. Statistics were done employing Fisher two-tailed tests. $^*p < 0.05$. ns, nonsignificant.

dysregulated in human primary airway cells from asthma patients. Integrating differentially expressed microRNAs and mRNAs determines that altered microRNA expression impacts the detected mRNA changes, underlying abnormalities relating to inflammation, glucocorticoid sensitivity, and epithelial repair detected by pathway analysis. This is affected through genome-wide modulation of mRNA levels and, most predominantly, through regulation of mRNA binding to polyribosomes. To our knowledge, ours is the first study to employ polyribosome profiling in human clinical samples and demonstrates that this approach reveals disease pathways and mRNA candidates not disclosed by other approaches, mainly transcriptomics, widely employed when studying human disease. For example, SA patients with an earlier disease onset clustered differently than those with later onset (Fig. 3) in the Polysome fraction. Although more numbers are needed to confirm this observation, it is consistent with reports suggesting that early- and late-onset SA represent stratified types of asthma with different etiologies (46). Polyribosome-bound mRNA analysis therefore highlights disease-related information overlooked by Total measurements and may serve as a novel tool to endotype patients, key in understanding and managing patients with complex diseases such as asthma and one of the hallmarks of personalized medicine.

One of the key advantages of Frac-seq is that it has more coverage (i.e., number of molecules revealed) than current proteomics approaches and informs about underlying molecular

Downloaded from http://www.jimmunol.org/ by guest on May 24, 2018

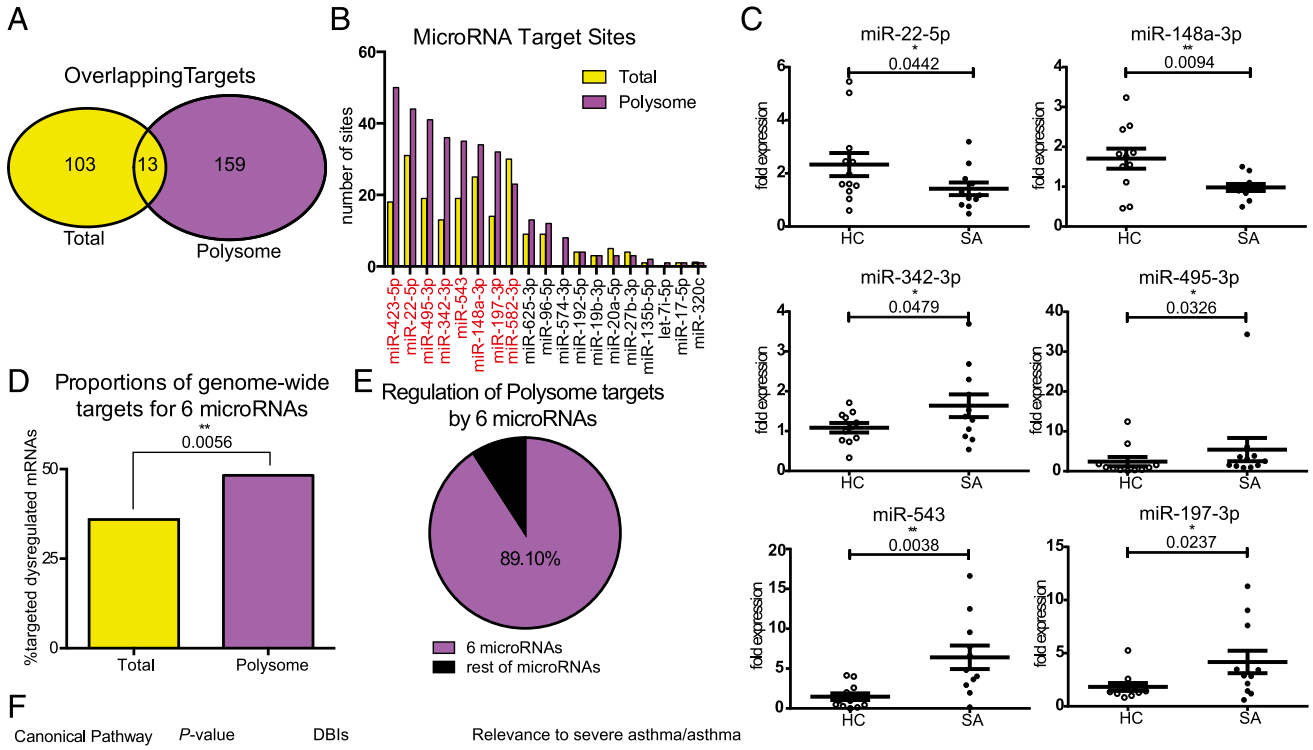

F

Canonical Pathway	*P*-value	DBIs	Relevance to severe asthma/asthma
Inositol Compounds	0.0212	DUSP1,IP6K1,IP6K2 MTMR2, MTMR9	INPP4A, a regulatory checkpoint in phosphoinositide signaling, is related to allergic airway inflammation (72)
Cell Cycle	0.00523	SMAD3,FOSL2,USP22 DUSP1,FOXC1,PDLIM7 ZNF703,GAS1,FGFRL1, IGFBP3,CDC27,KPNB1 EIF3M,PTP4A1	Asthmatic airway epithelium shows mitotic dyssynchrony (45); DUSP1 SNPs associated with clinical response to inhaled corticosteroids (63), implicated in glucocorticoid-dependent antiinflammatory effects (62) and reduced in SA animal model (73)

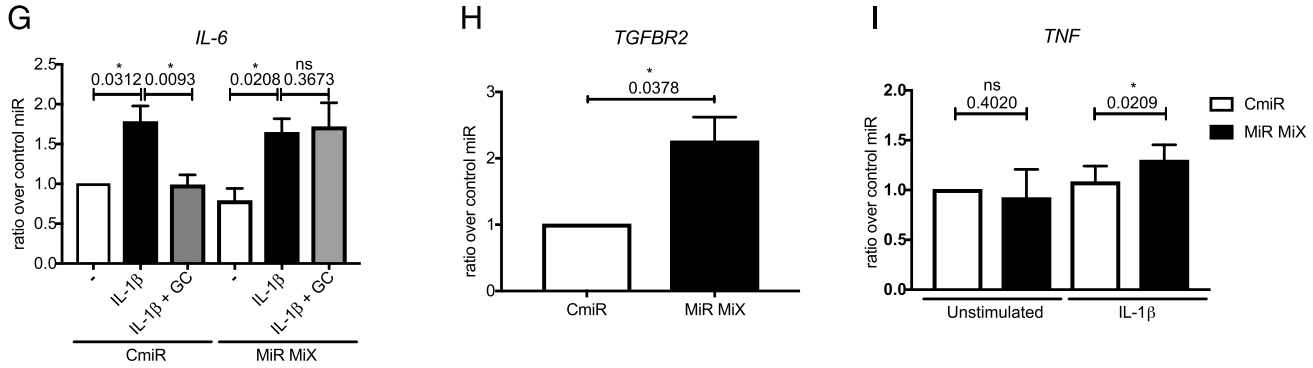

FIGURE 6. A subset of six microRNAs controls most of the mRNA targeting in SA bronchial epithelium. (**A**) Venn diagram depicting the overlap between total and polyribosome-bound microRNA targets by cross-referencing differentially expressed/bound isoforms with differentially expressed microRNAs in SA. (**B**) Bar plot depicting the number of targets for each differentially expressed microRNA in the Total (yellow) and Polysome (magenta) fractions. Highlighted in red are microRNAs with most abundant sites. (**C**) Dot plots (mean + SEM) representing qPCRs validating the subset of microRNAs among those with the highest number of targets in both fractions (n = 11 HC, n = 11 SA). Statistics were done employing t tests. (**D**) Bar plot depicting the proportional abundance of targets for the six validated microRNAs in Total (yellow) and Polysome (magenta) fractions. Polyribosome bound mRNAs have a higher abundance of microRNA targets (two-tailed Fisher exact test). (**E**) Pie chart depicting the proportion of targets among mRNAs controlled by microRNAs in the polyribosome-bound fraction that is potentially regulated by the validated six microRNAs. (**F**) Table showing the main asthma-related pathways predicted by IPA for mRNA DBIs and potentially targeted by the hub of six microRNAs. Red: upregulated; blue: downregulated. Statistics were done employing Fisher two-tailed test (72, 73). (**G–I**) Bar plots showing the results from transfecting the hub of six microRNAs (MiR MiX) compared with pre-microRNA and anti-microRNA controls at equimolar concentrations onto BECs from HCs. Forty-eight hours posttransfection cells were pretreated or not during 2 h with dexamethasone, stimulated or not with IL-1β, and harvested 24 h later. *$p < 0.05$, **$p < 0.01$. CmiR, control pre- and anti-microRNA mixture; MiR MiX, microRNA hub.

mechanisms of mRNA regulation, revealing mRNA isoforms preferentially bound to polyribosomes (20). Additionally, it reveals AS events that may lead to changes in 3′UTRs or 5′UTRs, which may not render differences in the amino acid sequence of proteins but strongly impact mRNA translation regulation. Expression changes in mRNAs undergoing translation revealed pathway abnormalities in SA relating to TLR signaling, the IL-1 pathway, and to p38 MAPK. Importantly, *IL1A* was detected as differentially translated and not transcribed (Fig. 3, Supplemental Fig. 2, respectively). These are all pathways distinct from those related to classical type 2 inflammation described in untreated steroid-responsive asthma (47) and mostly absent in our cohort

Downloaded from http://www.jimmunol.org/ by guest on May 24, 2018

(Supplemental Fig. 7). Moreover, the dysregulated microRNA network was found to regulate IL-1β responses in BECs (Fig. 6I), highlighting the intricate posttranscriptional dysregulation underlying disease characteristics in SA BECs.

Recent studies suggest that all human genes undergo AS, producing at least two alternative mRNA isoforms (19), with around 80% of AS events estimated to lead to protein modifications (48) and AS influencing protein output (21). Moreover, 25% of disease-related mutations have been linked to defects in splicing (49). If such changes existed in asthma, they could have profound and genome-wide implications in the proteins expressed by cells and, thus, in cellular function (21). The more in-depth analysis of mRNA DBIs identified, among other findings, defective signaling related to epithelial repair/remodeling pathways (e.g., Calpain protease or Paxillin signaling), supporting evidence from other approaches that there is an altered epithelial repair phenotype in SA (10, 50). These results are also supported by increased binding to polyribosomes of *ITGA2* and *ITGA6* mRNA isoforms in SA (Fig. 5), integrins being key adhesion and signaling proteins in the barrier (40).

The relevance and implications of employing Frac-seq in human clinical samples are also supported by previous findings at the protein level. The identification of increased epithelial polyribosomal *EGFR* mRNA binding in SA (Supplemental Fig. 8) supports the reported increased epithelial expression of Egfr protein (51). This has been attributed to a repair phenotype promoted by TGFβ-induced cell cycle inhibition (52). The present finding of increased binding to polyribosomes of *TGFBR2* (Supplemental Fig. 8), the main epithelial receptor for TGFβ, regulated by the microRNA hub (Fig. 6H), would underlie this potential. Bacterial products induce inflammatory responses via EGFR- and TLR-mediated pathways (53), with TLR-signaling present in pathways altered in Polysome, and viruses and bacteria exploiting Egfr to facilitate their survival (54, 55) or to attenuate the host response (56). Increased *IL23A*, *IL31R*, and *IL1A* translation in the epithelium would be consistent with an immune system orientated toward type I– and type 17–directed inflammation (Supplemental Fig. 7), more characteristic of a bacterial driven process, as would be the TLR pathway activation, phagosome formation, and the evidence of altered *IL6* isoforms binding to polyribosomes as well as IL-6 signaling in DBIs (Supplemental Datasets 7 and 8).

The translation of genes linked to innate immune responses raises the possibility that they arise in response to the altered airway microbiome in SA (57). An altered airway microbiome may also contribute to steroid resistance, one of the features of SA. Patients with SA suffer from persistent disease despite use of maximum therapy, including high doses of glucocorticoids. In the current study, glucocorticoid signaling was detected in Total (Supplemental Datasets 2 and 6), suggesting that corticosteroids are effectively reaching the airways of these patients and indicating that the lack of effect of steroid treatment is not a reflection of lack of adherence to treatment. Consideration needs to be given as to whether some of the differential expression changes in SA reflect steroid treatment. This does not appear the case for microRNAs as previous in vivo studies have reported that glucocorticoids have little effect on microRNA expression in bronchial epithelium (58, 59). Whereas steroids affect mRNA expression, there was no overlap between the identified upregulated genes in Total or Polysome, and gene changes described from previous genome-wide studies aimed at determining the effect of corticoids on gene expression (60, 61). Thus, the majority of described differential gene changes are likely to reflect alterations related to the underlying disease pathophysiology rather than directly because of their current therapy. Although glucocorticoid signaling was evident in Total, no glucocorticoid signaling was detectable in the polyribosome-associated pathways. *DUSP1* was identified as downregulated in SA, whereas several studies have highlighted the importance of this in glucocorticoid anti-inflammatory effects (62, 63). Indeed, we found that the microRNA network ablated the inhibition by glucocorticoids of IL-1β–driven IL-6 mRNA expression (Fig. 6G), potentially mimicking SA insensitivity to corticosteroids. IL-6 and IL-8 are typical inflammatory cytokines that are expressed by BECs and inhibited by glucocorticoids (64) and are upregulated in the airways of patients with SA (65). We also tested IL-8 mRNA expression, which showed a similar pattern but was nonstatistically significant (data not shown). Thus, in SA, there are nonsteroid responsive pathways evident within the bronchial epithelium mRNA translational signature and regulated by the hub of six microRNAs. These results may relate with the reported studies showing microRNAs not being affected by corticosteroid treatment and our results showing their preferential role in translation in asthma (Fig. 6). Together, these data highlight the need for the development of additional or alternative approaches to therapy in these patients and the importance of using polyribosome profiling to reveal novel pathophysiological mechanisms of potential implications in other inflammatory diseases, as previously implied in cancer (66).

Integrating small RNA expression allowed us to associate changes between mRNA and microRNA levels. Although previous studies have demonstrated the relevance of individual microRNAs in disease and particularly in asthma (67–69), there are no genome-wide studies addressing the relationship of microRNA levels with cytoplasmic and translational mRNA changes in asthma and, to our knowledge, in any other disease employing human clinical samples. Our results show that microRNA effects mostly rely on a hub of six microRNAs that potentially regulates ∼50% of all dysregulated mRNAs undergoing translation and ∼35% of cytoplasmic mRNA changes detected in asthma patients. We considered 6-, 7-, and 8-mer MREs, consistent with previous studies showing that all these contribute to target abundance (70). Our results are also consequent with microRNAs affecting both mRNA degradation (4, 24) and translation inhibition (2, 5). Recent work showing the relevance of ribosome binding for microRNA action (5), as well as mRNA degradation happening cotranslationally (71), supports our observation that microRNAs preferentially modulate mRNAs bound to polyribosomes. We could not find a relationship between the number of mRNA targets and the expression levels of the dysregulated microRNAs, as previously noted by Dessi et al. (66) in neuroblastoma. miR-148a-3p, with the highest expression in healthy individuals, and miR-197-3p, with the highest expression in asthmatic individuals, had the fewest number of mRNA targets among the hub of six microRNAs. Our results add novelty on a broad spectrum of biological contexts, as we have considered physiological changes in microRNA and mRNA levels in disease, rather than studying the isolated behavior of individual microRNAs or target mRNAs. In this context, microRNAs seem to target different mRNA populations when analyzing cytoplasmic or polyribosome-bound mRNAs (Fig. 6). We cannot exclude the possibility that inhibition of translation may have precluded cytoplasmic changes due to decay (4), or indeed, that some of the upregulation observed for microRNA targets may be due not only to a release of inhibition from microRNAs downregulated but also to transcriptional activation. Our data were obtained at one given time for both cytoplasmic and polyribosomal compartments together with the cytoplasmic microRNAome, considering mRNA physiological levels and supporting a preferential role for microRNAs in regulating mRNA translation and driving a disease phenotype in BECs

Downloaded from http://www.jimmunol.org/ by guest on May 24, 2018

(Fig. 6). Our validations place these microRNAs as key players in regulating SA characteristics, such as steroid refractoriness and inflammation. This is likely due to targeting of multiple signaling molecules in these pathways at the level of mRNA translation, such as *DUSP1*. Our results add to the latest studies demonstrating the intricate relationship between ribosome binding and mRNA fate with regards to stability and microRNA action.

In conclusion, our work demonstrates that although translation and AS are well-controlled processes in health, they are dysregulated genome-wide in asthma patients and that microRNAs account for many of the observed mRNA changes. This study reveals a new role for microRNAs in controlling impaired translation in asthma of potential implications in other inflammatory-related diseases, placing a hub of six microRNAs as potential future therapeutic candidates to address steroid-unresponsive epithelial activation in asthma. Our approach demonstrates the feasibility and added value of studying posttranscriptional gene regulation when investigating human biology and disease.

Acknowledgments

We thank the asthmatic and healthy participants who voluntarily participated in the research and the nursing support from the Southampton National Institute for Health Research Respiratory Biomedical Research Unit and Southampton Centre for Biomedical Research that enabled the study. We thank Prof. Mariana Castells, Dr. Christopher Woelk, Dr. Yawwani P. Gunawardana, Dr. Jeremy R. Sanford, Dr. Aishwarya Griselda Jacob, and Dr. Michael Breen for critical input to the article. We thank Dr. Michael Breen for statistical and computational analysis advice and Dr. Jeongmin Woo for advice in R. We thank Dr. Michael Edwards for help with the experiments to test microRNA effects.

Disclosures

Prof. Howarth reports personal fees from GlaxoSmithKline, outside the submitted work. The other authors have no financial conflicts of interest.

References

1. Bartel, D. P. 2009. MicroRNAs: target recognition and regulatory functions. *Cell* 136: 215–233.
2. Bazzini, A. A., M. T. Lee, and A. J. Giraldez. 2012. Ribosome profiling shows that miR-430 reduces translation before causing mRNA decay in zebrafish. *Science* 336: 233–237.
3. Djuranovic, S., A. Nahvi, and R. Green. 2012. miRNA-mediated gene silencing by translational repression followed by mRNA deadenylation and decay. *Science* 336: 237–240.
4. Eichhorn, S. W., H. Guo, S. E. McGeary, R. A. Rodriguez-Mias, C. Shin, D. Baek, S. H. Hsu, K. Ghoshal, J. Villén, and D. P. Bartel. 2014. mRNA destabilization is the dominant effect of mammalian microRNAs by the time substantial repression ensues. *Mol. Cell* 56: 104–115.
5. Tat, T. T., P. A. Maroney, S. Chamnongpol, J. Coller, and T. W. Nilsen. 2016. Cotranslational microRNA mediated messenger RNA destabilization. *Elife* 5: e12880.
6. Rupaimoole, R., and F. J. Slack. 2017. MicroRNA therapeutics: towards a new era for the management of cancer and other diseases. *Nat. Rev. Drug Discov.* 16: 203–222.
7. Martinez-Nunez, R. T., V. P. Bondanese, F. Louafi, A. S. Francisco-Garcia, H. Rupani, N. Bedke, S. Holgate, P. H. Howarth, D. E. Davies, and T. Sanchez-Elsner. 2014. A microRNA network dysregulated in asthma controls IL-6 production in bronchial epithelial cells. *PLoS One* 9: e111659.
8. Nunez-Iglesias, J., C. C. Liu, T. E. Morgan, C. E. Finch, and X. J. Zhou. 2010. Joint genome-wide profiling of miRNA and mRNA expression in Alzheimer's disease cortex reveals altered miRNA regulation. *PLoS One* 5: e8898.
9. Chung, K. F., S. E. Wenzel, J. L. Brozek, A. Bush, M. Castro, P. J. Sterk, I. M. Adcock, E. D. Bateman, E. H. Bel, E. R. Bleecker, et al. 2014. International ERS/ATS guidelines on definition, evaluation and treatment of severe asthma. [Published erratum appears in 2014 *Eur. Respir. J.* 43: 1216.] *Eur. Respir. J.* 43: 343–373.
10. Holgate, S. T., G. Roberts, H. S. Arshad, P. H. Howarth, and D. E. Davies. 2009. The role of the airway epithelium and its interaction with environmental factors in asthma pathogenesis. *Proc. Am. Thorac. Soc.* 6: 655–659.
11. Lambrecht, B. N., and H. Hammad. 2012. The airway epithelium in asthma. *Nat. Med.* 18: 684–692.
12. Piccirillo, C. A., E. Bjur, I. Topisirovic, N. Sonenberg, and O. Larsson. 2014. Translational control of immune responses: from transcripts to translatomes. *Nat. Immunol.* 15: 503–511.
13. Larsson, O., B. Tian, and N. Sonenberg. 2013. Toward a genome-wide landscape of translational control. *Cold Spring Harb. Perspect. Biol.* 5: a012302.
14. Gygi, S. P., Y. Rochon, B. R. Franza, and R. Aebersold. 1999. Correlation between protein and mRNA abundance in yeast. *Mol. Cell. Biol.* 19: 1720–1730.
15. Gunawardana, Y., S. Fujiwara, A. Takeda, J. Woo, C. Woelk, and M. Niranjan. 2015. Outlier detection at the transcriptome-proteome interface. *Bioinformatics* 31: 2530–2536.
16. Gunawardana, Y., and M. Niranjan. 2013. Bridging the gap between transcriptome and proteome measurements identifies post-translationally regulated genes. *Bioinformatics* 29: 3060–3066.
17. Zarai, Y., M. Margaliot, and T. Tuller. 2016. On the ribosomal density that maximizes protein translation rate. [Published erratum appears in 2017 *PLoS One* 12: e0177650.] *PLoS One* 11: e0166481.
18. Vogel, C., and E. M. Marcotte. 2012. Insights into the regulation of protein abundance from proteomic and transcriptomic analyses. *Nat. Rev. Genet.* 13: 227–232.
19. Lee, Y., and D. C. Rio. 2015. Mechanisms and regulation of alternative pre-mRNA splicing. *Annu. Rev. Biochem.* 84: 291–323.
20. Sterne-Weiler, T., R. T. Martinez-Nunez, J. M. Howard, I. Cvitovik, S. Katzman, M. A. Tariq, N. Pourmand, and J. R. Sanford. 2013. Frac-seq reveals isoform-specific recruitment to polyribosomes. *Genome Res.* 23: 1615–1623.
21. Floor, S. N., and J. A. Doudna. 2016. Tunable protein synthesis by transcript isoforms in human cells. *Elife* 5: e10921.
22. Martinez-Nunez, R. T., and J. R. Sanford. 2016. Studying isoform-specific mRNA recruitment to polyribosomes with Frac-seq. *Methods Mol. Biol.* 1358: 99–108.
23. Filipowicz, W., and N. Sonenberg. 2015. The long unfinished march towards understanding microRNA-mediated repression. *RNA* 21: 519–524.
24. Guo, H., N. T. Ingolia, J. S. Weissman, and D. P. Bartel. 2010. Mammalian microRNAs predominantly act to decrease target mRNA levels. *Nature* 466: 835–840.
25. Grainge, C. L., L. C. Lau, J. A. Ward, V. Dulay, G. Lahiff, S. Wilson, S. Holgate, D. E. Davies, and P. H. Howarth. 2011. Effect of bronchoconstriction on airway remodeling in asthma. *N. Engl. J. Med.* 364: 2006–2015.
26. Crowley, C., P. Klanrit, C. R. Butler, A. Varanou, M. Platé, R. E. Hynds, R. C. Chambers, A. M. Seifalian, M. A. Birchall, and S. M. Janes. 2016. Surface modification of a POSS-nanocomposite material to enhance cellular integration of a synthetic bioscaffold. *Biomaterials* 83: 283–293.
27. Langmead, B., and S. L. Salzberg. 2012. Fast gapped-read alignment with Bowtie 2. *Nat. Methods* 9: 357–359.
28. Kozomara, A., and S. Griffiths-Jones. 2014. miRBase: annotating high confidence microRNAs using deep sequencing data. *Nucleic Acids Res.* 42: D68–D73.
29. Ingolia, N. T. 2014. Ribosome profiling: new views of translation, from single codons to genome scale. *Nat. Rev. Genet.* 15: 205–213.
30. Heyer, E. E., and M. J. Moore. 2016. Redefining the translational status of 80S monosomes. *Cell* 164: 757–769.
31. Li, H., and R. Durbin. 2009. Fast and accurate short read alignment with Burrows-Wheeler transform. *Bioinformatics* 25: 1754–1760.
32. Li, B., and C. N. Dewey. 2011. RSEM: accurate transcript quantification from RNA-Seq data with or without a reference genome. *BMC Bioinformatics* 12: 323.
33. Benjamini, Y., and Y. Hochberg. 1995. Controlling the false discovery rate: a practical and powerful approach to multiple testing. *J. R. Stat. Soc. Ser. B* 57: 289–300.
34. Agarwal, V., G. W. Bell, J. W. Nam, and D. P. Bartel. 2015. Predicting effective microRNA target sites in mammalian mRNAs. *Elife* 4: e05005.
35. Querec, T. D., R. S. Akondy, E. K. Lee, W. Cao, H. I. Nakaya, D. Teuwen, A. Pirani, K. Gernert, J. Deng, B. Marzolf, et al. 2009. Systems biology approach predicts immunogenicity of the yellow fever vaccine in humans. *Nat. Immunol.* 10: 116–125.
36. Willson, T. M., and S. A. Kliewer. 2002. PXR, CAR and drug metabolism. *Nat. Rev. Drug Discov.* 1: 259–266.
37. Pascussi, J. M., L. Drocourt, J. M. Fabre, P. Maurel, and M. J. Vilarem. 2000. Dexamethasone induces pregnane X receptor and retinoid X receptor-alpha expression in human hepatocytes: synergistic increase of CYP3A4 induction by pregnane X receptor activators. *Mol. Pharmacol.* 58: 361–372.
38. Bezemer, G. F., S. Sagar, J. van Bergenhenegouwen, N. A. Georgiou, J. Garssen, A. D. Kraneveld, and G. Folkerts. 2012. Dual role of Toll-like receptors in asthma and chronic obstructive pulmonary disease. *Pharmacol. Rev.* 64: 337–358.
39. Gao, P., P. G. Gibson, K. J. Baines, I. A. Yang, J. W. Upham, P. N. Reynolds, S. Hodge, A. L. James, C. Jenkins, M. J. Peters, et al. 2015. Anti-inflammatory deficiencies in neutrophilic asthma: reduced galectin-3 and IL-1RA/IL-1β. *Respir. Res.* 16: 5.
40. Harburger, D. S., and D. A. Calderwood. 2009. Integrin signalling at a glance. [Published erratum appears in 2009 *J. Cell Sci.* 122: 1472.] *J. Cell Sci.* 122: 159–163.
41. Park, C. S. 2010. Eosinophilic bronchitis, eosinophilia associated genetic variants, and notch signaling in asthma. *Allergy Asthma Immunol. Res.* 2: 188–194.
42. Albrecht, E., E. Sillanpää, S. Karrasch, A. C. Alves, V. Codd, I. Hovatta, J. L. Buxton, C. P. Nelson, L. Broer, S. Hägg, et al. 2014. Telomere length in circulating leukocytes is associated with lung function and disease. *Eur. Respir. J.* 43: 983–992.
43. Al-Muhsen, S., J. R. Johnson, and Q. Hamid. 2011. Remodeling in asthma. *J. Allergy Clin. Immunol.* 128: 451–462; quiz 463–464.
44. Sandberg, R., J. R. Neilson, A. Sarma, P. A. Sharp, and C. B. Burge. 2008. Proliferating cells express mRNAs with shortened 3′ untranslated regions and fewer microRNA target sites. *Science* 320: 1643–1647.

Downloaded from http://www.jimmunol.org/ by guest on May 24, 2018

45. Freishtat, R. J., A. M. Watson, A. S. Benton, S. F. Iqbal, D. K. Pillai, M. C. Rose, and E. P. Hoffman. 2011. Asthmatic airway epithelium is intrinsically inflammatory and mitotically dyssynchronous. *Am. J. Respir. Cell Mol. Biol.* 44: 863–869.
46. Haldar, P., I. D. Pavord, D. E. Shaw, M. A. Berry, M. Thomas, C. E. Brightling, A. J. Wardlaw, and R. H. Green. 2008. Cluster analysis and clinical asthma phenotypes. *Am. J. Respir. Crit. Care Med.* 178: 218–224.
47. Woodruff, P. G., H. A. Boushey, G. M. Dolganov, C. S. Barker, Y. H. Yang, S. Donnelly, A. Ellwanger, S. S. Sidhu, T. P. Dao-Pick, C. Pantoja, et al. 2007. Genome-wide profiling identifies epithelial cell genes associated with asthma and with treatment response to corticosteroids. *Proc. Natl. Acad. Sci. USA* 104: 15858–15863.
48. Modrek, B., and C. Lee. 2002. A genomic view of alternative splicing. *Nat. Genet.* 30: 13–19.
49. Sterne-Weiler, T., J. Howard, M. Mort, D. N. Cooper, and J. R. Sanford. 2011. Loss of exon identity is a common mechanism of human inherited disease. *Genome Res.* 21: 1563–1571.
50. Loxham, M., D. E. Davies, and C. Blume. 2014. Epithelial function and dysfunction in asthma. *Clin. Exp. Allergy* 44: 1299–1313.
51. Puddicombe, S. M., R. Polosa, A. Richter, M. T. Krishna, P. H. Howarth, S. T. Holgate, and D. E. Davies. 2000. Involvement of the epidermal growth factor receptor in epithelial repair in asthma. *FASEB J.* 14: 1362–1374.
52. Puddicombe, S. M., C. Torres-Lozano, A. Richter, F. Bucchieri, J. L. Lordan, P. H. Howarth, B. Vrugt, R. Albers, R. Djukanovic, S. T. Holgate, et al. 2003. Increased expression of p21(waf) cyclin-dependent kinase inhibitor in asthmatic bronchial epithelium. *Am. J. Respir. Cell Mol. Biol.* 28: 61–68.
53. Koff, J. L., M. X. Shao, I. F. Ueki, and J. A. Nadel. 2008. Multiple TLRs activate EGFR via a signaling cascade to produce innate immune responses in airway epithelium. *Am. J. Physiol. Lung Cell. Mol. Physiol.* 294: L1068–L1075.
54. Monick, M. M., K. Cameron, J. Staber, L. S. Powers, T. O. Yarovinsky, J. G. Koland, and G. W. Hunninghake. 2005. Activation of the epidermal growth factor receptor by respiratory syncytial virus results in increased inflammation and delayed apoptosis. *J. Biol. Chem.* 280: 2147–2158.
55. Subauste, M. C., and D. Proud. 2001. Effects of tumor necrosis factor-alpha, epidermal growth factor and transforming growth factor-alpha on interleukin-8 production by, and human rhinovirus replication in, bronchial epithelial cells. *Int. Immunopharmacol.* 1: 1229–1234.
56. Mikami, F., H. Gu, H. Jono, A. Andalibi, H. Kai, and J. D. Li. 2005. Epidermal growth factor receptor acts as a negative regulator for bacterium nontypeable *Haemophilus influenzae*-induced Toll-like receptor 2 expression via an Src-dependent p38 mitogen-activated protein kinase signaling pathway. *J. Biol. Chem.* 280: 36185–36194.
57. Green, B. J., S. Wiriyachaiporn, C. Grainge, G. B. Rogers, V. Kehagia, L. Lau, M. P. Carroll, K. D. Bruce, and P. H. Howarth. 2014. Potentially pathogenic airway bacteria and neutrophilic inflammation in treatment resistant severe asthma. *PLoS One* 9: e100645.
58. Moschos, S. A., A. E. Williams, M. M. Perry, M. A. Birrell, M. G. Belvisi, and M. A. Lindsay. 2007. Expression profiling in vivo demonstrates rapid changes in lung microRNA levels following lipopolysaccharide-induced inflammation but not in the anti-inflammatory action of glucocorticoids. *BMC Genomics* 8: 240.
59. Solberg, O. D., E. J. Ostrin, M. I. Love, J. C. Peng, N. R. Bhakta, L. Hou, C. Nguyen, M. Solon, C. Nguyen, A. J. Barczak, et al. 2012. Airway epithelial miRNA expression is altered in asthma. *Am. J. Respir. Crit. Care Med.* 186: 965–974.
60. Reddy, T. E., F. Pauli, R. O. Sprouse, N. F. Neff, K. M. Newberry, M. J. Garabedian, and R. M. Myers. 2009. Genomic determination of the glucocorticoid response reveals unexpected mechanisms of gene regulation. *Genome Res.* 19: 2163–2171.
61. Yick, C. Y., A. H. Zwinderman, P. W. Kunst, K. Grünberg, T. Mauad, K. Fluiter, E. H. Bel, R. Lutter, F. Baas, and P. J. Sterk. 2013. Glucocorticoid-induced changes in gene expression of airway smooth muscle in patients with asthma. *Am. J. Respir. Crit. Care Med.* 187: 1076–1084.
62. Abraham, S. M., T. Lawrence, A. Kleiman, P. Warden, M. Medghalchi, J. Tuckermann, J. Saklatvala, and A. R. Clark. 2006. Antiinflammatory effects of dexamethasone are partly dependent on induction of dual specificity phosphatase 1. *J. Exp. Med.* 203: 1883–1889.
63. Jin, Y., D. Hu, E. L. Peterson, C. Eng, A. M. Levin, K. Wells, K. Beckman, R. Kumar, M. A. Seibold, G. Karungi, et al. 2010. Dual-specificity phosphatase 1 as a pharmacogenetic modifier of inhaled steroid response among asthmatic patients. *J Allergy Clin Immunol.* 126: 618–625.e1–2.
64. Levine, S. J., P. Larivée, C. Logun, C. W. Angus, and J. H. Shelhamer. 1993. Corticosteroids differentially regulate secretion of IL-6, IL-8, and G-CSF by a human bronchial epithelial cell line. *Am. J. Physiol.* 265: L360–L368.
65. Morjaria, J. B., K. S. Babu, P. Vijayanand, A. J. Chauhan, D. E. Davies, and S. T. Holgate. 2011. Sputum IL-6 concentrations in severe asthma and its relationship with FEV1. *Thorax* 66: 537.
66. Dassi, E., V. Greco, V. Sidarovich, P. Zuccotti, N. Arseni, P. Scaruffi, G. P. Tonini, and A. Quattrone. 2015. Translational compensation of genomic instability in neuroblastoma. *Sci. Rep.* 5: 14364.
67. Haj-Salem, I., R. Fakhfakh, J. C. Bérubé, E. Jacques, S. Plante, M. J. Simard, Y. Bossé, and J. Chakir. 2015. MicroRNA-19a enhances proliferation of bronchial epithelial cells by targeting TGFβR2 gene in severe asthma. *Allergy* 70: 212–219.
68. Kim, R. Y., J. C. Horvat, J. W. Pinkerton, M. R. Starkey, A. T. Essilfie, J. R. Mayall, P. M. Nair, N. G. Hansbro, B. Jones, T. J. Haw, et al. 2017. MicroRNA-21 drives severe, steroid-insensitive experimental asthma by amplifying phosphoinositide 3-kinase-mediated suppression of histone deacetylase 2. *J. Allergy Clin. Immunol.* 139: 519–532.
69. Maes, T., F. A. Cobos, F. Schleich, V. Sorbello, M. Henket, K. De Preter, K. R. Bracke, G. Conickx, C. Mesnil, J. Vandesompele, et al. 2016. Asthma inflammatory phenotypes show differential microRNA expression in sputum. *J. Allergy Clin. Immunol.* 137: 1433–1446.
70. Denzler, R., S. E. McGeary, A. C. Title, V. Agarwal, D. P. Bartel, and M. Stoffel. 2016. Impact of microRNA levels, target-site complementarity, and cooperativity on competing endogenous RNA-regulated gene expression. *Mol. Cell* 64: 565–579.
71. Pelechano, V., W. Wei, and L. M. Steinmetz. 2015. Widespread co-translational RNA decay reveals ribosome dynamics. *Cell* 161: 1400–1412.
72. Aich, J., U. Mabalirajan, T. Ahmad, A. Agrawal, and B. Ghosh. 2012. Loss-of-function of inositol polyphosphate-4-phosphatase reversibly increases the severity of allergic airway inflammation. *Nat. Commun.* 3: 877.
73. Gauthier, M., T. Oriss, M. Raundhal, C. Morse, S. E. Wenzel, P. Ray, and A. Ray. 2016. A potential mechanism for steroid resistance in severe asthma. Am. J. Respir. Crit. Care Med. 193: A7771 (Abstr).

Downloaded from http://www.jimmunol.org/ by guest on May 24, 2018

SUPPLEMENTAL DATA

Genome-wide post-transcriptional dysregulation by microRNAs in human asthma as revealed by Frac-seq

Rocio T. Martinez-Nunez, Hitasha Rupani, Manuela Platé, Mahesan Niranjan, Rachel C. Chambers, Peter H. Howarth and Tilman Sanchez-Elsner

Correspondence to: rocio.martinez_nunez@kcl.ac.uk

This document contains:

Supplemental Table 1.

Supplemental Table 2.

Supplemental Table 3.

Supplemental Table 4.

Supplemental Figure 1.

Supplemental Figure 2.

Supplemental Figure 3.

Supplemental Figure 4.

Supplemental Figure 5.

Supplemental Figure 6.

Supplemental Figure 7.

Supplemental Figure 8.

Characteristic	HC	SA	*P*-value
Number	11	11	
Age	42 (24-64)	50 (21-75)	0.1961
Sex, M/F	6/5	4/7	0.6699
FEV1, %predicted	104(82.8-137)	55(40-96)	<0.0001
BMI	25.66(20.51-38.78)	27.53(22.56-44.91)	0.2105
Atopy, n (%)	2(18)	7(64)	0.0805
GINA treatment step 4(n)/5(n)	N/A	8/3	
ACQ score	N/A	3.6(1.4-5.29)	
Age of onset	N/A	40(3-63)	
ICS dose, BDP equivalent, mg	N/A	1880(800-3800)	
Number on oral steroids	N/A	6	
BAL cell differential			
% macrophages	89.5(53-97)	80.5(27.75-95.37)	0.0418
% neutrophils	0.63(0.25-4.5)	3.5(0.25-24.25)	0.0149
% eosinophils	0.125(0-0.63)	1.125(0-9.3)	0.0244

Supplemental Table 1
Table showing the patient demographics of the samples employed in our Frac-seq study (RNA-seq and validations). M: male. F: Female. FEV_1: Forced Expiratory Volume in 1 second. BMI: Body Mass Index. ACQ: Asthma Control Questionnaire. ICS: Inhaled CorticoSteroids. BDP: Beclometasone DiPropionate CFC. BAL: BronchoAlveolar Lavage. Displayed are median values with minimum and maximum values in parentheses unless otherwise noted. n: number of subjects.

Mature microRNA	Tukey *P*-value	BH-*P*-value	Ratio (SA/HC)	Average HC	Average SA
hsa-miR-127-3p	0.00209	0.0438375	3.2807	94.3095	309.401
hsa-miR-582-3p	0.00842	0.0438375	0.50825	201.456	102.391
hsa-miR-543	0.00888	0.0438375	1.96735	94.3095	185.54
hsa-miR-495-3p	0.0105	0.0438375	2.12373	103.526	219.861
hsa-miR-17-5p	0.0114	0.0438375	0.62905	2336.76	1469.93
hsa-miR-135b-5p	0.01301	0.0438375	0.44881	582.853	261.592
hsa-miR-320c	0.01634	0.0438375	1.73803	376.489	654.35
hsa-miR-27b-3p	0.0167	0.0438375	0.59625	25116.8	14975.9
hsa-miR-192-5p	0.02748	0.048444375	0.53322	340.871	181.761
hsa-miR-99b-5p	0.02904	0.048444375	1.64847	22861.8	37687.1
hsa-miR-20a-5p	0.03184	0.048444375	0.40933	4159.58	1702.64
hsa-let-7i-5p	0.03263	0.048444375	0.51429	28019.3	14410
hsa-miR-148a-3p	0.03312	0.048444375	0.5045	23895.9	12055.5
hsa-miR-574-3p	0.03521	0.048444375	1.99342	645.447	1286.65
hsa-miR-342-3p	0.03562	0.048444375	1.86156	121.649	226.457
hsa-miR-22-5p	0.03691	0.048444375	0.65288	511.41	333.888
hsa-miR-96-5p	0.04065	0.04861	0.53342	354.725	189.216
hsa-miR-625-3p	0.04257	0.04861	1.78649	209.069	373.499
hsa-miR-197-3p	0.04656	0.04861	1.59589	2757.42	4400.53
hsa-miR-423-5p	0.04738	0.04861	1.86581	5127.81	9567.53
hsa-miR-19b-3p	0.04861	0.04861	0.48168	398.76	192.075

Supplemental Table 2
Results of our small RNA-seq. MicroRNAs differentially expressed between healthy controls and severe asthmatic bronchial epithelial cells. Detection threshold for healthy controls and severe asthmatics: 35.28 and 63.17, respectively. HC: Healthy Control. SA: Severe Asthma. BH-*P*-value: Benjamini-Hochberg corrected *P*-value.

Diseases and Disorders	p-value range	#Molecules
Cancer	4.57E-02 - 2.24E-09	15
Organismal Injury (*) and Abnormalities	4.66E-02 - 2.24E-09	18
Inflammatory Response	3.67E-02 - 5.30E-09	9
Hematological Disease	4.39E-02 - 1.14E-08	10
Immunological Disease	4.39E-02 - 1.14E-08	9
Molecular and Cellular Functions	**p-value range**	**#Molecules**
Cellular Development	2.59E-02 - 1.20E-06	8
Cellular Growth and Proliferation	2.04E-02 - 1.20E-06	8
Cellular Movement	1.09E-02 - 9.45E-04	4
Cell Cycle	2.64E-02 - 2.80E-03	3
Cell Morphology	2.80E-03 - 2.80E-03	1
Top Networks	**Score**	
Cancer, Organismal Injury and Abnormalities, Reproductive System Disease	29	
Cellular Development, Cellular Growth and Proliferation, Cell Cycle	2	
Hereditary Disorder, Inflammatory Disease, Inflammatory Response	2	
Cellular Movement, Cell Morphology, Digestive System Development and Function	2	

Supplemental Table 3
Ingenuity Pathway Analysis results for the 20 microRNAs dysregulated in severe asthma bronchial epithelium as compared to healthy control. P value ranges correspond to multiple pathways converging in the mentioned disorders, functions and networks. Note that (*) is referred to as "repair" in the main text.

Diseases and Disorders	**p-value range**	**#Molecules**
Cancer	4.99E-02 - 6.21E-04	132
Organismal Injury (*) and Abnormalities	4.99E-02 - 6.21E-04	132
Reproductive System Disease	4.92E-02 - 6.21E-04	41
Infectious Disease	2.13E-02 - 1.39E-03	4
Gastrointestinal Disease	4.30E-02 - 1.85E-03	118
Molecular and Cellular Functions	**p-value range**	**#Molecules**
Cell Cycle	4.91E-02 - 1.04E-03	17
Cellular Movement	4.22E-02 - 1.39E-03	6
Carbohydrate Metabolism	4.91E-02 - 5.03E-03	7
Lipid Metabolism	4.91E-02 - 5.03E-03	7
Small Molecule Biochemistry	4.91E-02 - 5.03E-03	14
Top 10 Canonical Pathways	**p-value**	**Overlap**
Inositol Pyrophosphates Biosynthesis	1.04E-03	28.6% (2/7)
Cholesterol Biosynthesis I	3.77E-03	15.4% (2/13)
Cholesterol Biosynthesis II (via 24,25-dihydrolanosterol)	3.77E-03	15.4% (2/13)
Cholesterol Biosynthesis III (via Desmosterol)	3.77E-03	15.4% (2/13)
Mitotic Roles of Polo-Like Kinase	1.04E-02	4.8% (3/63)
Epoxysqualene Biosynthesis	1.43E-02	50% (1/2)
Superpathway of Cholesterol Biosynthesis	1.59E-02	7.4% (2/27)
Superpathway of Inositol Phosphate Compounds	2.12E-02	2.3% (5/220)
Heme degradation	2.84E-02	25% (1/4)
Role of Oct4 in Mammalian Embryonic Stem Cell Pluripotency	4.13E-02	4.4% (2/45)

Supplemental Table 4
IPA analysis of microRNA targets in the polyribosome-bound fraction for the hub of 6 microRNAs. P value ranges correspond to multiple pathways converging in the mentioned disorders, functions and networks. Note that (*) is referred to as "repair" in the main text.

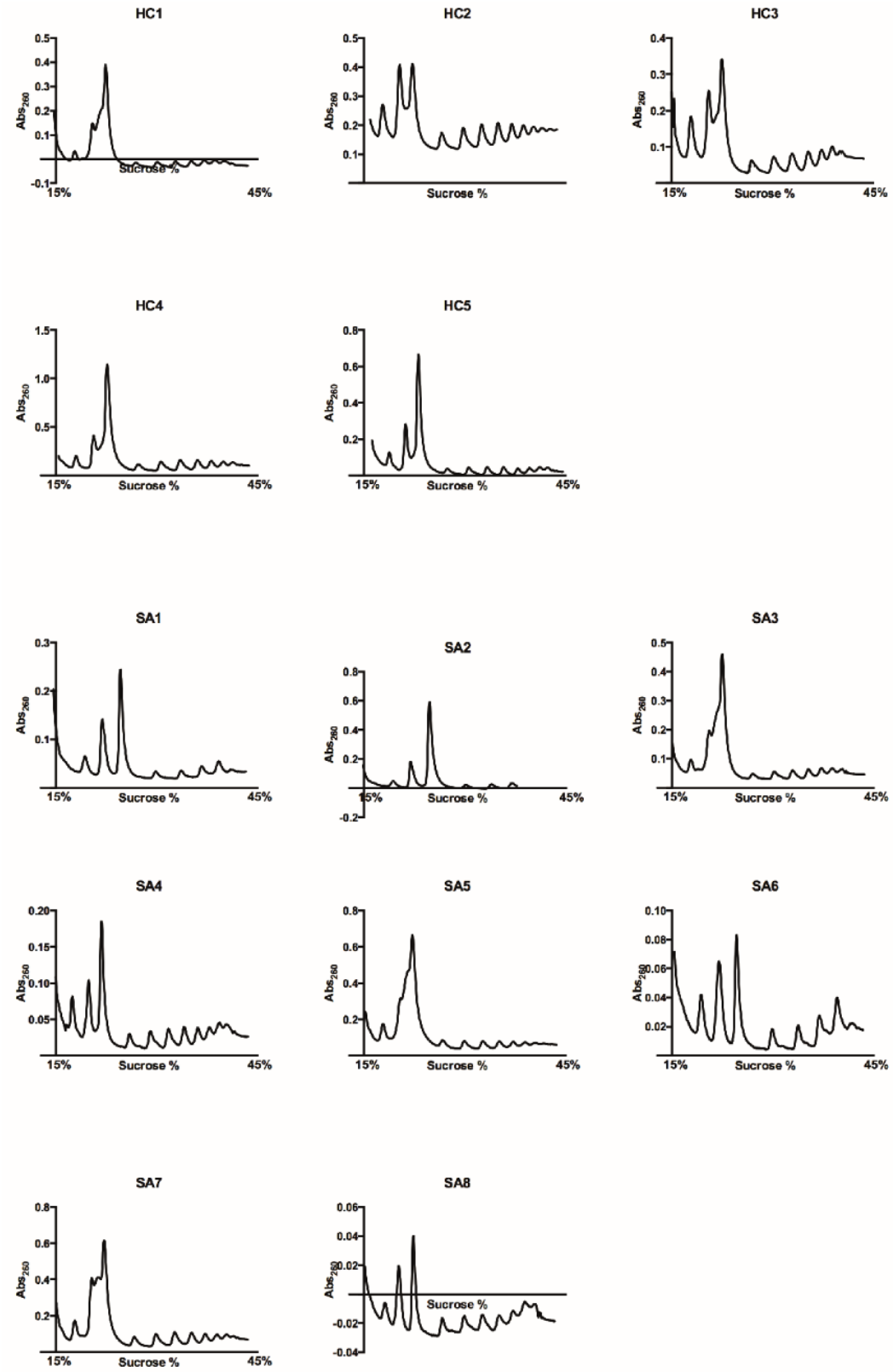

Supplemental Figure 1.
Polyribosome profiles of the bronchial epithelial cells sequenced. Graphs showing the polyribosomal profiles of the volunteers in our study.

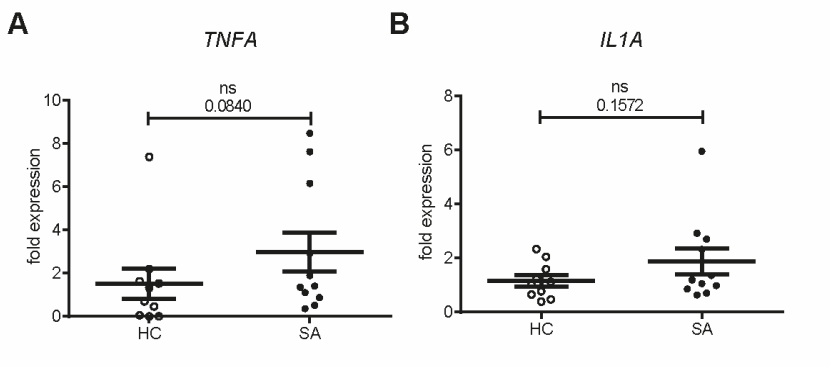

Supplemental Figure 2.
A. Differentially expressed gene in Total mRNA tested that was not validated in our bigger cohort. Note that *P* value bordered statistical significance (HC = 10, SA = 11). **B**. *IL1A* did not show differential expression between health and disease, confirming our RNA-seq data (HC = 10, SA = 11).

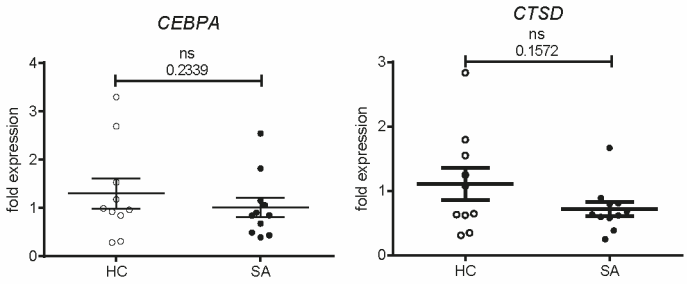

Supplemental Figure 3
Differentially expressed genes in Polysome mRNA tested that were not validated in our bigger cohort (n=10 HC, n=11 SA).

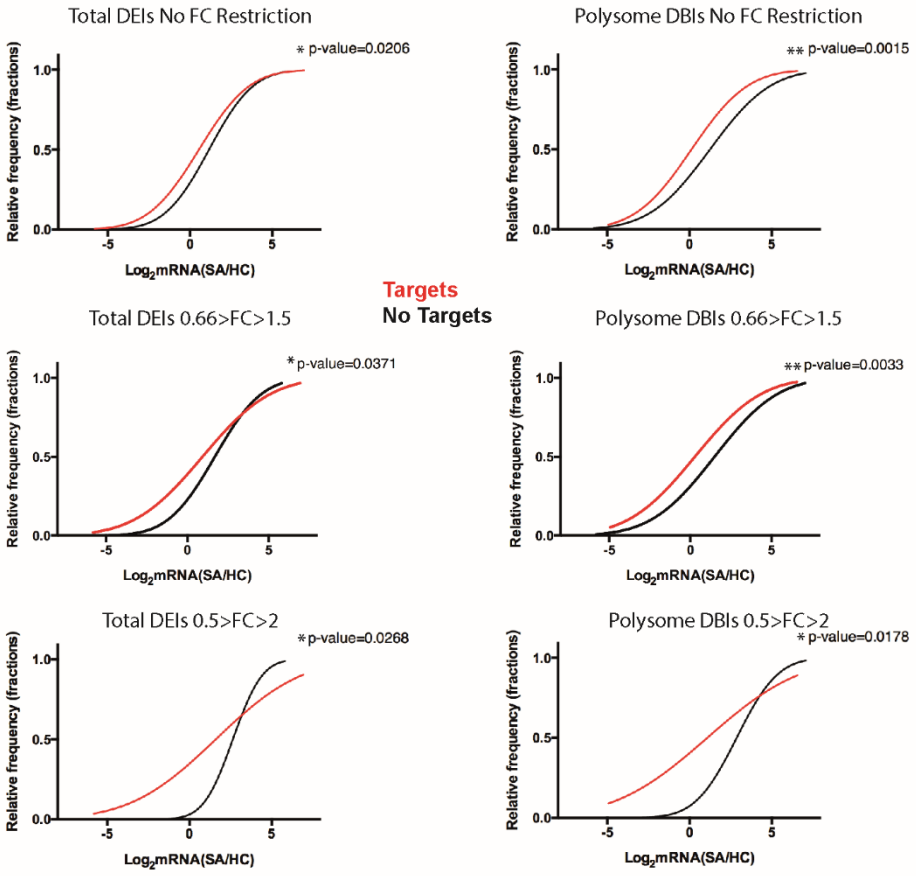

Supplemental Figure 4
MicroRNA targeting of mRNAs in Total and Polysome fractions. Cumulative distributions of mRNA changes for differentially expressed isoforms between severe asthma and healthy controls, comparing Targets vs No Targets for microRNAs in our dataset. For both Total (left panels) and polyribosome bound mRNAs (right panels), we changed the parameters for inclusion in the analysis concerning ratio SA/HC ($P < 0.01$) mRNA fold changes (FC). From considering no restriction (top row) to considering 0.66>FC>1.5 (middle row) or a more restrictive 0.5>FC>2 (bottom row), the distribution of mRNA changes between targets and no-targets significantly changed (Kolmogorov-Smirnov test) in all cases. These data strengthen our results regarding microRNA effects, showing that they are not dependent on the mRNA fold changes considered in the analysis.

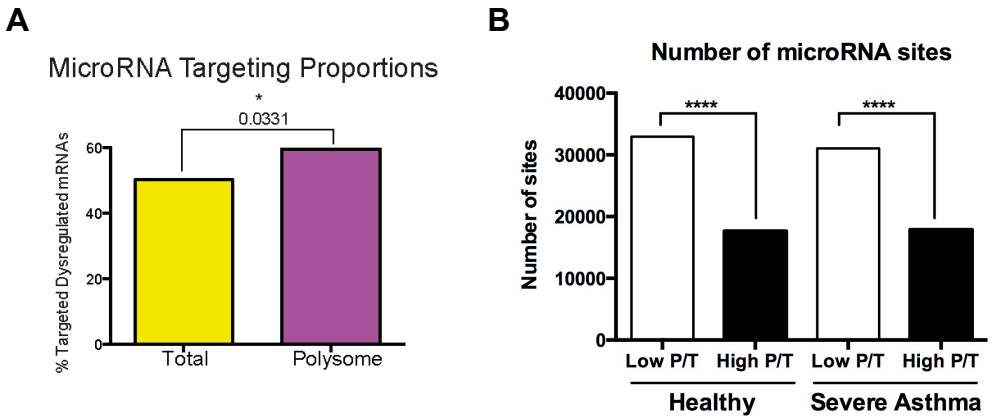

Supplemental Figure 5
A: Proportions of mRNAs targeted by the 20 dysregulated microRNAs in the Total (yellow) and Polysome (magenta) fractions. Statistics were done employing Fisher's exact test. **B:** Number of microRNA sites according to subcellular localization. MicroRNA binding sites were sought in the top and bottom 10% mRNA isoforms (3084 mRNAs on each) according to their normalised mean expression values of polyribosome/total ratio. Gene IDs of those isoforms were then cross-referenced with the predicted conserved targets of conserved microRNAs from TargetScan database 7.0. mRNAs with high polyribosome/total ratios (High P/T) showed significantly less microRNA binding sites than low polyribosome/total mRNAs. These data are consistent with microRNAs inhibiting mRNA translation (as association with polyribosomes). Statistics were performed in R employing χ^2 goodness-of-fit test with equal expected frequencies.

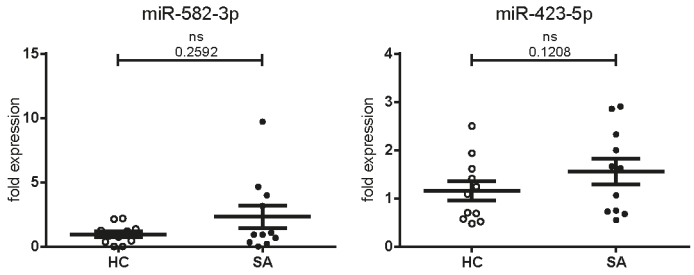

Supplemental Figure 6
MicroRNAs not validated in our bigger cohort of donors (n=11 HC and n=11 SA). MicroRNA miR-582 was barely detectable by qPCR.

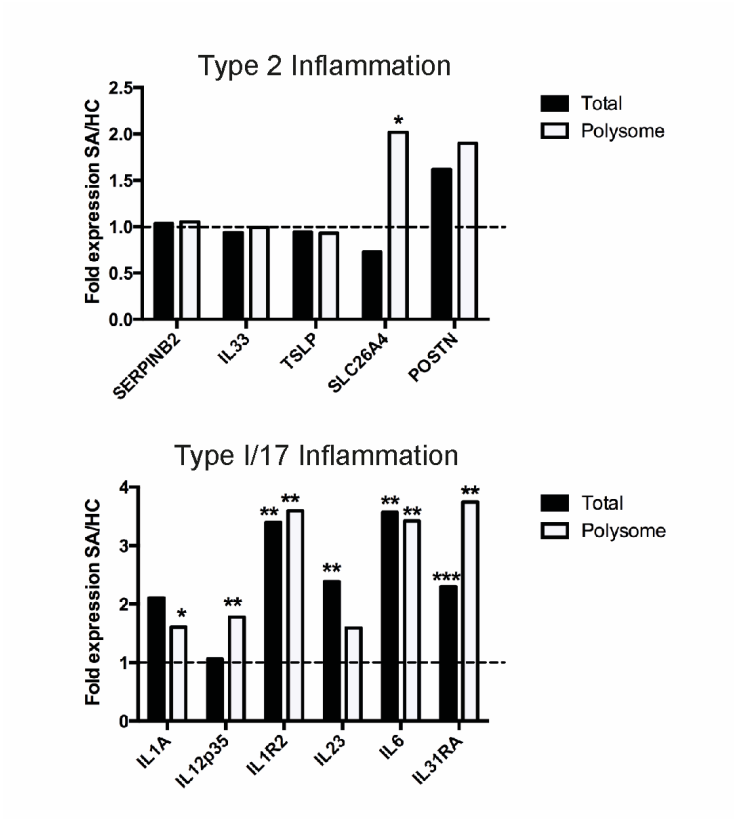

Supplemental Figure 7
Fold change (SA/HC) of epithelial cell markers characteristic of type 2 inflammation (upper graph) and type 1/17 inflammation (lower graph) according to our RNA-seq results. P values correspond to comparing healthy vs severe asthma. *: $P \leq 0.05$; **: $P \leq 0.01$, ***: $P \leq 0.001$.

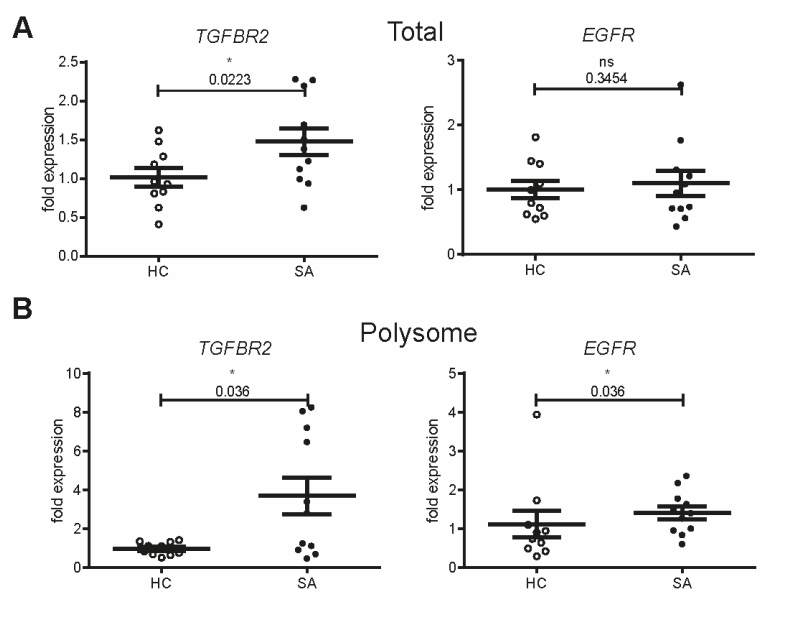

Supplemental Figure 8
qPCR expression data for *TGFBR2* and *EGFR* in the total cytoplasmic fraction (upper graphs, **A**) and in the polyribosome-bound fraction (lower graphs, **B**) (n=10 HC, n=11 SA).

SUPPLEMENTAL INTERACTIVE FIGURES LEGENDS

Supplemental Interactive Figure 1. Network of interactions between the 6 microRNAs and their targets (gene ID of the isoforms) in the Total cytoplasmic fraction. Note the 2 subnetworks corresponding to microRNAs up-regulated and their down-regulated targets and *vice versa* (HTML).

Supplemental Interactive Figure 2. Network of interactions between the 6 microRNAs and their targets (gene ID of the isoforms) in polyribosome bound mRNAs. Note the 2 subnetworks corresponding to microRNAs up-regulated and their down-regulated targets and *vice versa*. The 2 subnetworks are connected via *GFOD1*, since this gene presents 2 differentially expressed isoforms (one up-regulated and one down-regulated) that share the same 3'UTR (HTML).